

Accelerator Development Department

BROOKHAVEN NATIONAL LABORATORY

Associated Universities, Inc.

Upton, New York 11973

SSC Technical Note No. 80

SSC-N-590

CONSTRUCTION, TEST AND DISASSEMBLY OF 17 m SSC DIPOLE DD0012

P. Wanderer, R. Coombes, A. Devred, C. Goodzeit

J. Kaugerts, K. Mirk, T. Nicol and J. Tompkins

February 18, 1989



CONSTRUCTION, TEST, AND DISASSEMBLY OF 17M SSC DIPOLE DD0012

P. Wanderer, R. Coombes, A. Devred, C. Goodzeit,  
J. Kaugerts, K. Mirk, T. Nicol, and J. Tompkins

February 18, 1989

REPORT OUTLINE

Overview (p. 3)

SECTION 1 - GENERAL DESCRIPTION AND ASSEMBLY

- I. Fabrication Highlights (p. 4)
- II. Instrumentation Description (p. 4)
  - A. Voltage taps
  - B. Coil Azimuthal Strain Gauges
  - C. End Plate Strain Gauges
  - D. Cold Mass Skin Gauges
  - E. End Motion Transducers
  - F. Extensometer
  - G. Pressure Transducer
- III. Magnetic Measurements at Room Temperature (p. 7)
  - A. Multipole measurements at BNL
  - B. Dipole angle measurements at Fermilab
- IV. Exceptions During Fabrication or Prior to Testing (p.

SECTION 2 -- MAGNETIC TESTS AT CRYOGENIC TEMPERATURES

- I. Summary of Test History (p. 9)
  - A. Discussion of Procedure
  - B. Overview of Tests
  
- II. Magnet Mechanics -- Strain Gauge Data. (p. 10)
  - A. Coil Azimuthal Strain Gauges
  - B. End Plate Stress Data
  - C. Cold Mass Skin Gauges
  - D. Extensometer
  - E. End Plate Motion Indicator
  
- III. Quench Behavior (p. 15)
  - A. Quench Currents
  - B. Quench Location
  - C. Associated Data (Spot Heaters, MIITs, Propagation Velocities)
  
- IV. Summary of Test Results. (p. 18)
  
- V. Exceptions during Testing (p. 19)
  - A. Rapid Quench Propagation in Non-quenching Quarter Coil
  - B. Unusual Behavior of Magnet Current Following Spot Heater Quench
  - C. Buss Voltage Pulses

SECTION 3 -- DISASSEMBLY AND INSPECTION (p. 22)

## I. Coil Size Data

## II. Inspection of Components

OVERVIEW

The construction features of this magnet were designed to significantly reduce axial and azimuthal coil motion during magnet excitation, relative to previous 17m dipoles. The main features were (1) shims between the yoke and collars and (2) thick end plates. The magnet was heavily instrumented with voltage taps (four per inner coil turn) so that the quench origin could be well-localized.

The quench performance of the magnet was very good. The first spontaneous quench of the magnet was at 6.52kA (6.6T), the limit of the conductor at 4.4K. The highest quench current was 7.64kA.

After testing, the magnet was disassembled and inspected. The only anomalies found were in the ramp-splice assembly, which had been identified by voltage tap data as the region of the magnet which most limited its performance at reduced helium temperature. When DD12 is reassembled, the ramp-splice will have a new design.

SECTION 1 -- GENERAL DESCRIPTION AND ASSEMBLYI. Fabrication Highlights.

The conductor used for the inner coils had a copper-to-superconductor ratio of 1.6, with 20 micron filament diameter. Similar material was used in 1.8m magnets DSS10-12. The variation of coil size along the magnet length was typical of coils made with this tooling (+- 4 mils for the inner layer, +- 3 mils for the outer layer). For both inner and outer windings, the average size of the upper was the same as the lower within 1 mil. The coils were made to the C358A cross section. After the coils were molded, gaps in the ends were filled with a mixture of alumina and epoxy.

The stainless steel, spot-welded collars used to assemble the coils used rectangular keys. Shims were placed between the collars and yoke. A brass shim 10 mils thick was used from the midplane to about 45 degrees. A stainless steel shim 15 mils thick covered the region from 45 degrees to the pole. (Availability dictated the choice of shim material.) A non-magnetic yoke was placed over the coil end and the last 2.5" of the inner layer straight section. After the shell was welded, the coil ends were prestressed axially to about 4000 pounds via pressure applied from the stainless steel end plates, which were 1.5" thick and not split at the midplane. The magnet was shipped to Fermilab on Jan 12, 1988.

II. Instrumentation.

#### A. Voltage Taps

During assembly, four voltage taps were placed on each turn of the inner layer, approximately 16" from the end of the coil straight section. The taps on the remainder of the magnet were the standard arrangement. The one exception to this was the addition of separate taps (and a separate quench detection circuit) to the buss. The rewiring for the buss taps was made during the course of the magnet test.

#### B. Coil Azimuthal Strain Gauges

The magnet used the new BNL beam-type gauges in both inner and outer coils. Four separate gauges were used to measure the stress of each layer. The gauges were located where the inner coils were smallest, about 51" from the lead end. Compensating gauges were also installed.

#### C. End Plate Strain Gauges

The end plate at the non-lead end of the magnet was instrumented with four bullet-type force transducers. Each transducer had two strain gauges on it. The same end plate also had two strain gauges epoxied to it, so that a comparison could be made with data from a similar gauge epoxied to the end plate at the lead end of the magnet. (Space limitations at the lead end prevented the use of bullets there.) Temperature compensating gauges were also provided.

#### D. Cold Mass Skin Gauges

Eleven strain gauges were epoxied to the cold mass skin, oriented so that they would measure axial strain. (Each "gauge" on the skin is actually a pair at the same axial position, but 180 degrees apart azimuthally.) They were 30, 40, 50, and 80 inches from the non-lead end and 10, 20, 30, 40, 50, 80 inches from the lead end. A gauge was mounted at the axial center, 331 inches from the ends. Two strain gauges were epoxied to the cold mass skin in the orientation for measuring azimuthal strain. One gauge was 81" from the lead end, the other was the same distance from the non-lead end.

#### E. End Motion Transducers ("Niemann Gauges")

An end motion transducer was added to the lead end of the cold mass at Fermilab. The transducer is a G10 rod which is spring-loaded against the end plate and monitored by a transverse beam which has a strain gauge mounted on it. Motion of the rod deflects the beam and the resultant strain induced is used to measure the motion. The transducer monitors the motion of the end plate, the collars, and the yoke with respect to the bonnet. It was recorded dynamically as well as in the periodic Cryolog file.

#### F. Extensometer

An unrestrained, 17m-long, 304 stainless steel rod was mounted on the outside of the s.s. shell, and pushed against the actuator of a 2" long linear potentiometer at the return end. The extensometer measured the differential length change between the rod and the cold mass assembly. The material of

the rod was the same as the shell material; however, the shell developed a two-dimensional strain pattern that affected its length.

#### G. Pressure Transducer

In addition to the pressure transducers in each of the end cans, the magnet had a cold pressure transducer at its axial center.

### III. Magnetic Measurements at Room Temperature

#### A. Multipole, Dipole Angle Measurements at BNL

After testing at Fermilab the cold mass was returned to BNL and mounted on an assembly fixture at room temperature. The magnetic field was then measured using the BNL mole. A number of caveats apply to these measurements, the most important being that no correction has been made for feeddown. The measured multipole field strength and dipole field angle, averaged over the magnet length, are given in Table 1.III.A.1. The Table contains z-averages for +10A, -10A, and the average of these two currents for one of the two runs. (Averages from the other run agree within a few hundredths of a unit.) For the +10A data only, the lowest order multipoles and the dipole angle are plotted against z in Figs. 1.III.A.1 and 1.III.A.2 (bottom half) respectively. A full report of the data is given in a separate report (BNL Magnet Test Group report TMG-390).



Magnet dd0012 coefficients averaged by program WARM. First line is avg., second line is rms var.

dd0012.203ck **(-10A)** 30-NOV-88 AVERAGE MULTIPOLE COEFFS. (UNITS) FOR RECORDS 1 THROUGH 56 AT 1.0 CM  
 26 measurements included in the average Data type=1 (1=+I warm; 2=-I warm; 3=up ramp; 4=down ramp) BZMIN=0.0090  
 DIPOLE FIELD ANGLE mean +- sigma = -0.61+- 4.36mrad CURRENT mean +- sigma = 10.00+- 0.01 AMPS

b0	b1	b2	b3	b4	b5	b6	b7	b8	b9	b10	b11	b12	b13	b14
1.00000	-1.86	-2.65	0.15	1.45	0.01	-0.23	0.00	0.09	0.00	0.07	0.00	-0.01	0.00	0.01
0.00000	2.13	0.64	0.15	0.08	0.04	0.02	0.02	0.01	0.01	0.00	0.00	0.00	0.00	0.00
a0	a1	a2	a3	a4	a5	a6	a7	a8	a9	a10	a11	a12	a13	a14
0.00000	2.62	-0.04	0.23	0.19	0.10	0.01	-0.03	0.01	-0.03	0.01	0.01	0.00	-0.01	0.00
0.00000	0.66	0.30	0.14	0.08	0.04	0.02	0.02	0.01	0.02	0.00	0.00	0.00	0.00	0.00

**(-10A)** dd0012.203ck 30-NOV-88 AVERAGE MULTIPOLE COEFFS. (UNITS) FOR RECORDS 1 THROUGH 56 AT 1.0 CM  
 26 measurements included in the average Data type=2 (1=+I warm; 2=-I warm; 3=up ramp; 4=down ramp) BZMIN=0.0090  
 DIPOLE FIELD ANGLE mean +- sigma = 3141.12+- 4.08mrad CURRENT mean +- sigma = -10.00+- 0.01 AMPS

b0	b1	b2	b3	b4	b5	b6	b7	b8	b9	b10	b11	b12	b13	b14
-1.00000	-1.88	7.00	-0.23	-1.06	-0.01	0.22	0.00	-0.09	0.00	-0.08	0.00	0.01	0.00	0.01
0.00000	2.57	0.42	0.16	0.09	0.04	0.02	0.01	0.01	0.01	0.00	0.00	0.00	0.00	0.00
a0	a1	a2	a3	a4	a5	a6	a7	a8	a9	a10	a11	a12	a13	a14
1.36564	-2.63	0.18	-0.32	-0.16	-0.10	-0.01	0.03	-0.01	0.03	-0.01	-0.01	0.00	0.01	0.00
2.83054	0.97	0.36	0.17	0.10	0.04	0.02	0.02	0.01	0.01	0.00	0.00	0.00	0.00	0.00

Results of warm-~~old~~ comparison for magnet dd0012 by program WARM run 1-DEC-88 at 16:38:54  
 dd0012.203ck is warm dsf

**AUG +, - 10A**

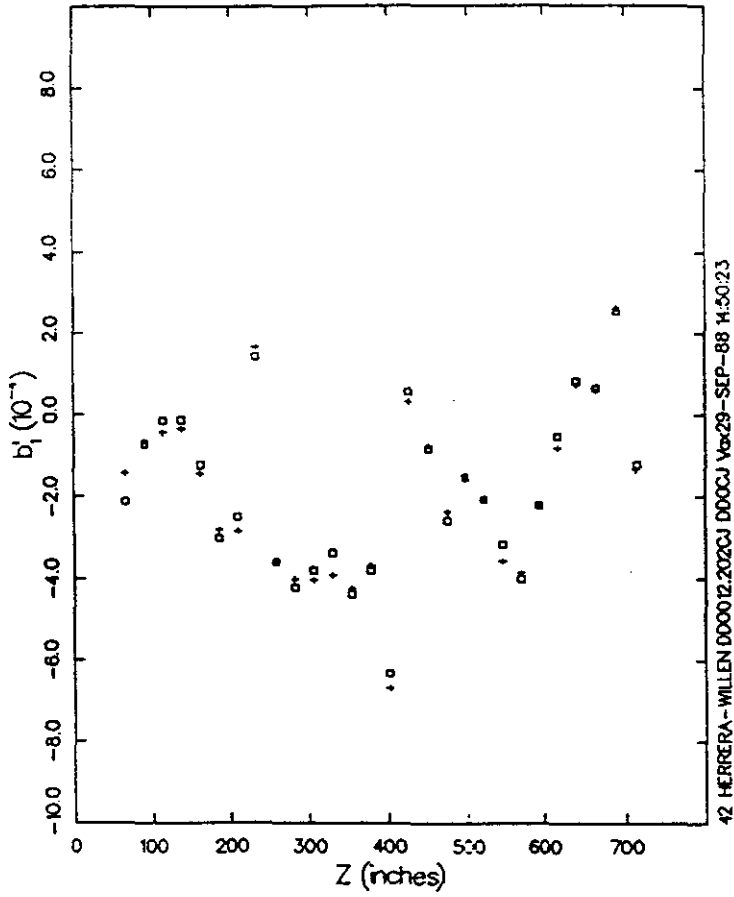
AVG. ANGLE = (-.61 - .47) / 2 = -0.54 mrad.

Normal terms  
 warm 1.00 0.01 -4.83 0.19 1.25 0.01 -0.22 0.00 0.09 0.00 0.07 0.00 -0.01 0.00 0.01

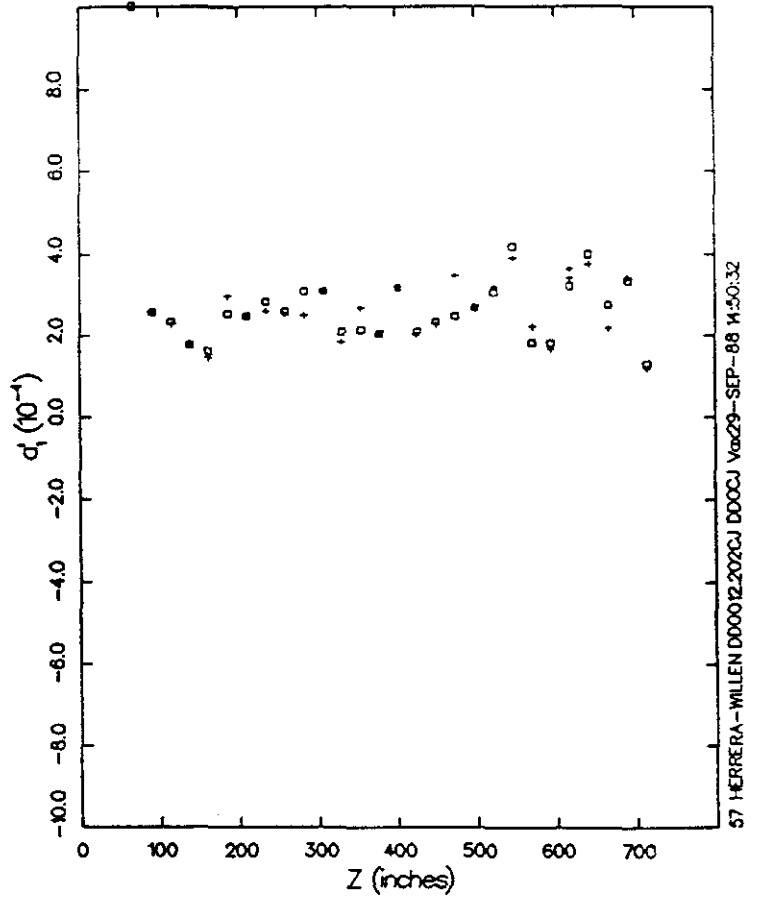
Skew terms  
 warm -0.68 2.63 -0.11 0.28 0.18 0.10 0.01 -0.03 0.01 -0.03 0.01 0.00 -0.01 0.00 0.00

Table 1.III.A.1

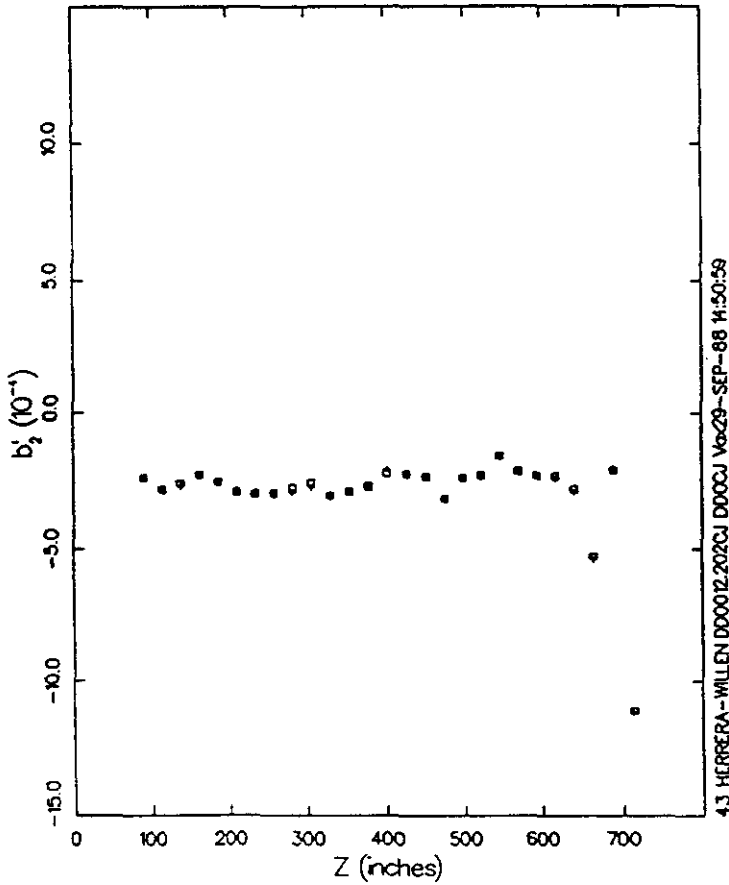
11 DD0012 Normal quadrupole fractional coefficient at  $r,cm=1.00$



12 DD0012 Skew quadrupole fractional coefficient at  $r,cm=1.00$



15 DD0012 Normal sextupole fractional coefficient at  $r,cm=1.00$



16 DD0012 Skew sextupole fractional coefficient at  $r,cm=1.00$

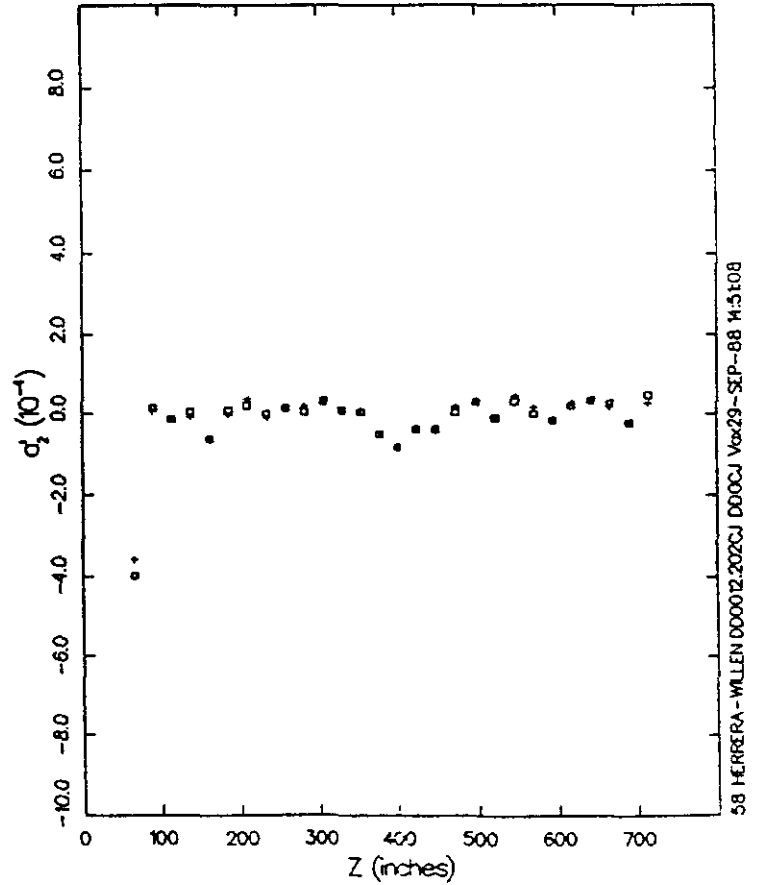


Fig. 1. III.A.1

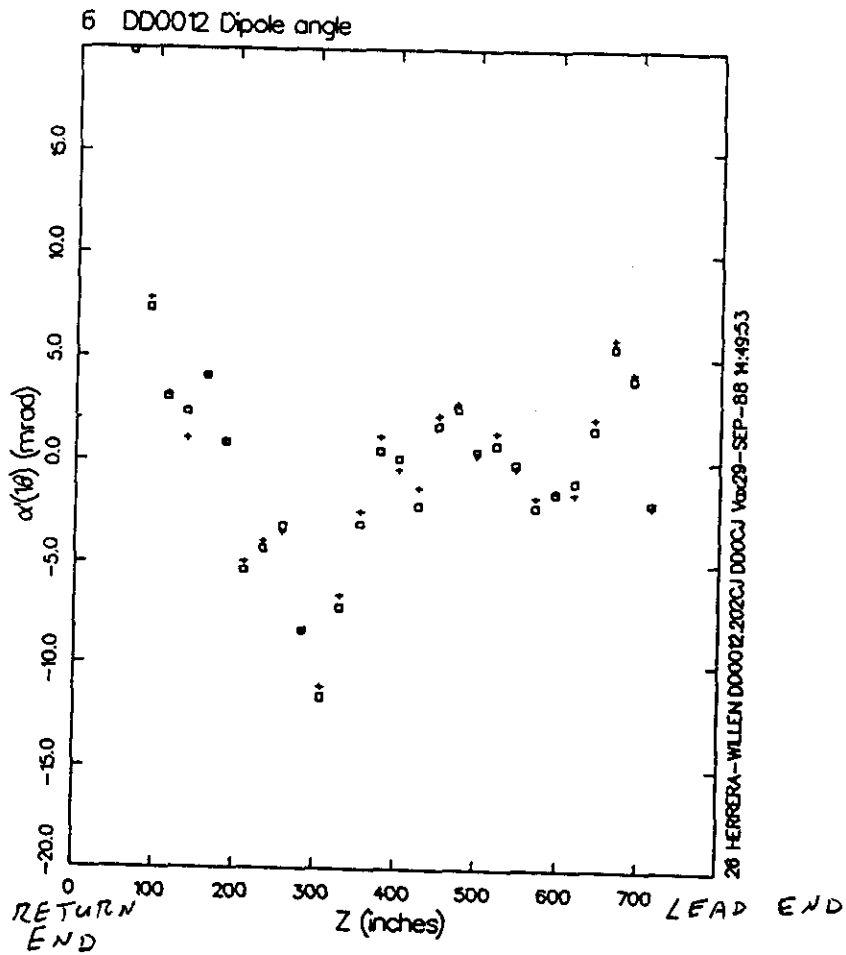
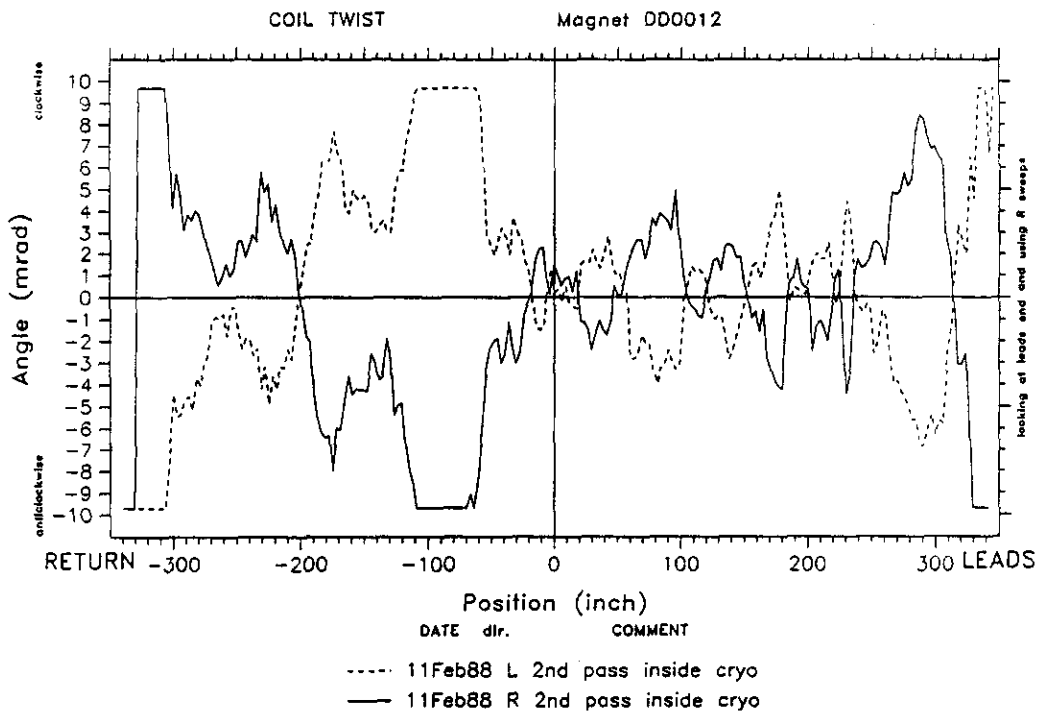


Fig. 1.III.A.2

## B. Dipole Angle Measurements at Fermilab

A measurement of the dipole angle was made at Fermilab after the cold mass had been mounted in the cryostat. These data are presented in Fig. 1.III.A.2 (top half). The BNL and Fermilab measurements are in good qualitative agreement, particularly in light of the fact that the BNL measurement was made with the cold mass on assembly fixturing, rather than in the cryostat.

## IV. Exceptions During Fabrication or Prior to Testing.

A turn-to-turn short between the two turns nearest the midplane at the end of the straight section of inner coil LLNI-18 was caused by the inward radial displacement of the midplane lead. After this short was repaired, these two turns again shorted together in the same region, just beyond the area covered by the repair of the original short. The cause of this second short was less clear-- it could have been due to the original displacement of the lead or due to a mismatch between the sizes of the end and straight section. (Sizing is much more precise on later magnets.) The repair of the second short (adding kapton; reducing shims) extended for 6" into the straight section, which was just beyond the ramp-splice area.

SECTION 2 -- MAGNET TESTS AT CRYOGENIC TEMPERATURESI. Summary of Test History.

## A. Discussion of Procedure

The test program followed fairly standard procedures. After cooldown and electrical checkout, the magnet current was increased stepwise so that strain gauge data could be taken. The first quench occurred on a strain gauge run. The magnet was then quenched several times to establish the plateau quench current. The magnet quench performance was also established at temperatures below the normal 4.35K operating temperature and after a thermal cycle. Spot heaters were used to initiate quenches in specific locations and at specific currents.

## B. Overview of Tests

The test program proceeded along the lines summarized in the previous section. The magnet was tested on Stand 5 and was able to take advantage of the lower helium temperatures available there. Quenching at low temperature during the first thermal cycle was ended when the refrigerator system became contaminated and was warmed up for cleaning. Testing took place during May and June 1988.

Testing was slowed by a number of problems. Voltage pulses from the buss (thought to be due to motion without quenching) gave false triggers to the quench detection circuitry. Eventually, the buss voltage was processed by a

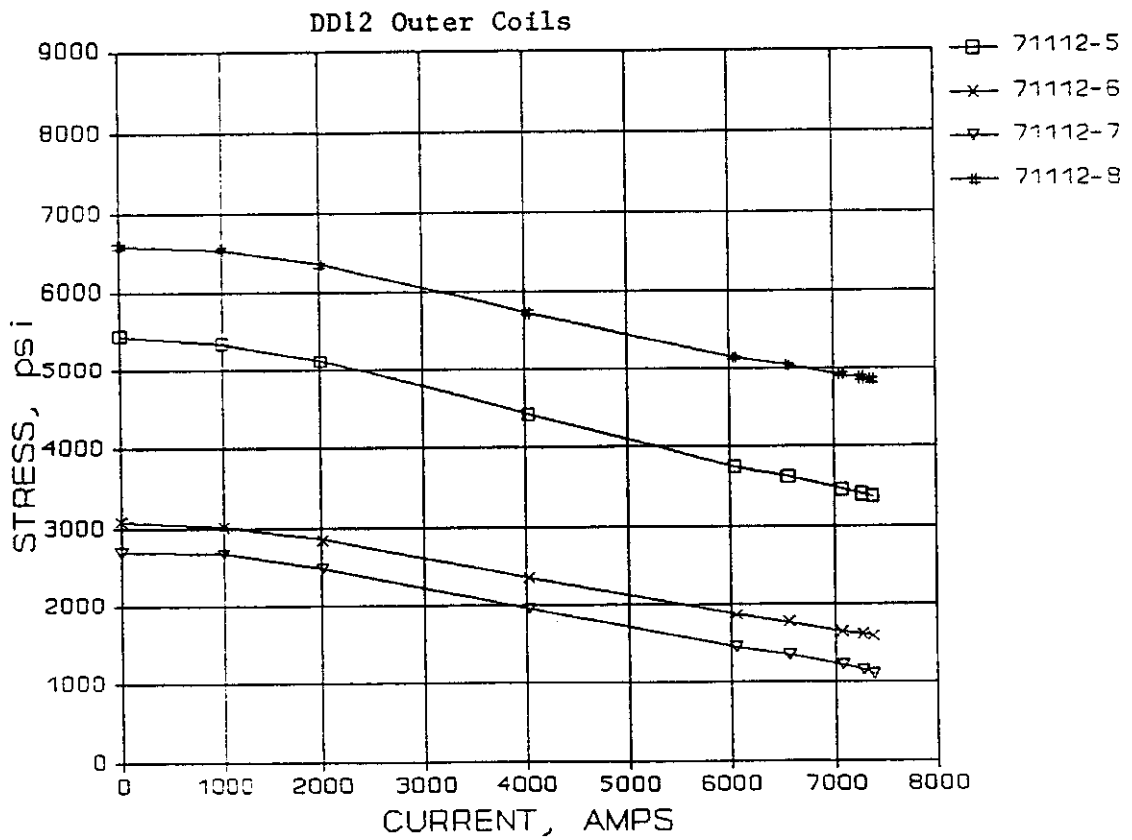
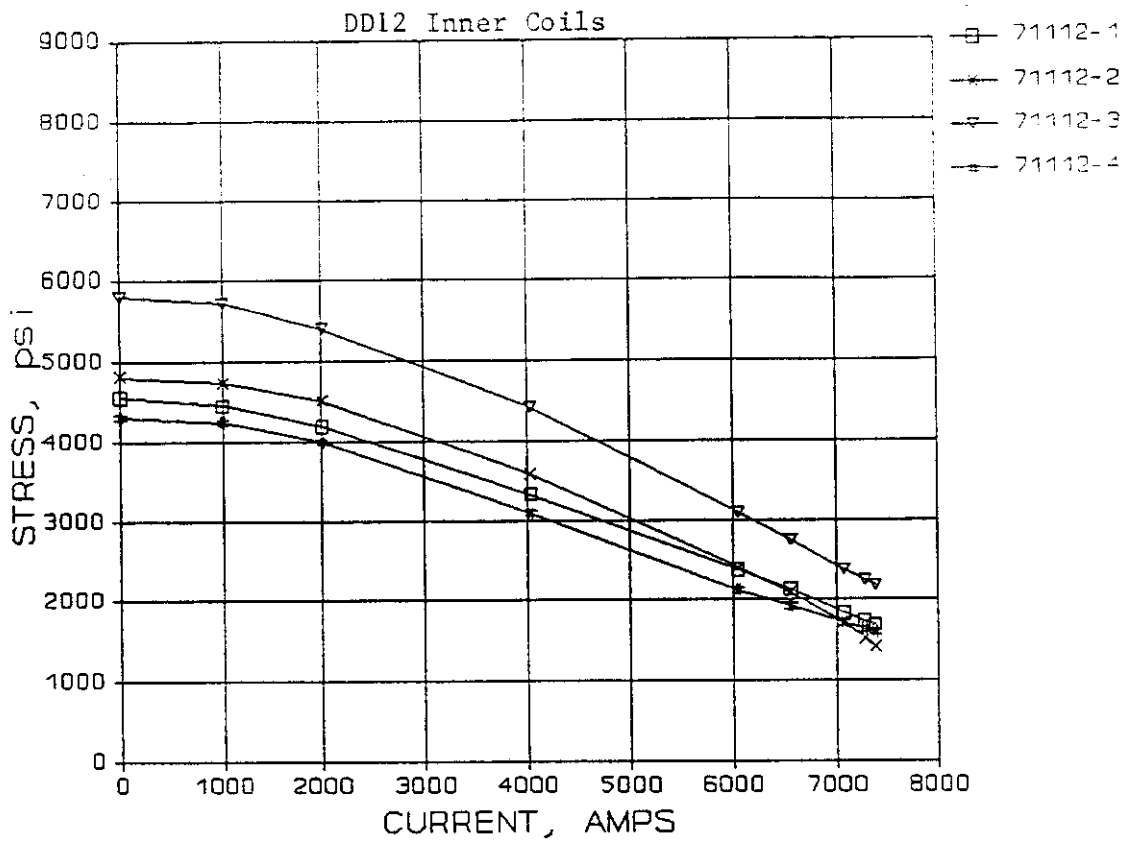


Fig. 2.II.A.1

separate circuit, which smoothed the signals before sending them to a quench detection circuit with a separate threshold. False quench triggers apparently due to random noise also occurred. The summer's heat, and consequent cooling problems, often restricted testing to evenings and nights. The record-high quench currents exceeded the capacity of the transducer used for power supply control, so a shunt was used instead.

## II. Magnet Mechanics (Strain Gauge Data).

### A. Coil Azimuthal Strain Gauges

Considerable effort was put into the development of accurate gauges for these measurements. The gauges in DD12 were the new BNL beam-type gauges. Data from the individual gauges are plotted against current in Fig. 2.II.A.1. The responses of the four inner coil gauges (top) are quite similar; the same is true of the four outer coil gauges. Further, at  $I=0$ , the four inner coil gauges are within 1 kpsi of 5 kpsi (i.e.,  $\pm 20\%$ ). There is more spread in the outer coil gauges. The differences could be in the gauges or in the magnet itself. (Gauges 1, 2, 5, 6 are in the upper coil half.)

The data in this report use 4.2K no-load constants measured after the magnet had been tested. The final calibrations differ from the initial ones in that the post-test 4.2K readings were made on the active and compensating gauges at the same time. The stresses calculated with the final

calibrations are 200 - 800 psi lower than those calculated with the initial values.

For coil azimuthal prestress, a simple statement of the design goal is that the coil have non-zero prestress at SSC operating current (6.5kA), with some margin. The prestress data shown in Fig. 2.II.A.1 and the prestress changes given in Table 2.II.A.1 indicate that both inner and outer coils had significant prestress at 7.4kA, the highest current for which data were taken. At this current, the magnet was not at the conductor limit, but was limited by quenches originating in the ramp-splice.

The average stress for the inner and outer coils is plotted against the square of the current in Fig. 2.II.A.2. The deviation from a straight line suggests elastic moduli which increase with current.

The complete history of the magnet is summarized in Table 2.II.A.2. Broadly speaking, the 0.8 kpsi drop of prestress in the inner coil from the time of assembly until disassembly at BNL may be due to creep. (Interestingly, the outer coil prestress increases 0.4 kpsi during the same period.) The inner coil cold prestress values show no significant change during either of the two periods of cold testing. (The same can be said for the outer coil values.) This is interesting because the inner coil prestress values dropped about 0.5 kpsi during the initial testing of the magnet (Fig. 2.II.A.3, which does not use the post-test 4.2K constants).

TOTAL AZIMUTHAL STRESS AND END FORCE CHANGE  
FROM STRAIN GAUGE RUN

TOTAL CURRENT CHANGE, amps	7369
71112-1, UI-RIGHT, psi	-2875
71112-2, UI-LEFT, psi	-3400
71112-3, LI-LEFT, psi	-3630
71112-4, LI-RIGHT, psi	-2719
AVERAGE INNER COILS, psi	-3156
71112-5, UO-RIGHT, psi	-2095
71112-6, UO-LEFT, psi	-1507
71112-7, LO-LEFT, psi	-1606
71112-8, LO-LEFT, psi	-1752
AVERAGE OUTER COILS, psi	-1740
71116-1, END FORCE, lbs	-1662
71116-2, END FORCE, lbs	-1553
71116-3, END FORCE, lbs	-1775
71116-4, END FORCE, lbs	-1342
TOTAL END FORCE, lbs	-6332

Table 2.II.A.1

DD0012 COIL STRESS AND END FORCE SUMMARY

DATE	STATUS	AVG. INNER	AVG. OUTER	TOTAL END FORCE	DELTA INNER	DELTA OUTER	DELTA END
12/17/87	After Collaring	7225	4822	0			
12/18/87	After Shell Welded	7469	5621	0	244	800	0
1/ 9/88	At FNAL	7319	5549	-1206	-150	-73	-1206
4/28/88	In Test Stand, Warm	7023	5155	-3935	-296	-393	-2729
5/ 1/88	In Test Stand, 4.4K	4998	4704	-4199	-2026	-452	-264
5/17/88	Prior to Warm-up	5185	4566	-5171	187	-138	-972
5/23/88	In Test Stand, Warm	6814	5439	-3616	1629	873	1555
6/10/88	In Test Stand, Warm	6675	5323	-3160	-139	-116	456
6/14/88	In Test Stand, 4.4K	4759	4697	-4073	-1916	-627	-913
6/21/88	Prior to Warm-up	5139	4568	-5226	380	-129	-1153
7/10/88	In Test Stand, Warm	6530	5475	-3216	1391	907	2010
9/15/88	At BNL	6438	5238	0	-92	-236	3216
10/11/88	After Shell Cutting	5650	4104	0	-789	-1135	0
10/11/88	Gauge Pack Removed	-11	63	0	-5661	-4040	0

Table 2.II.A.2

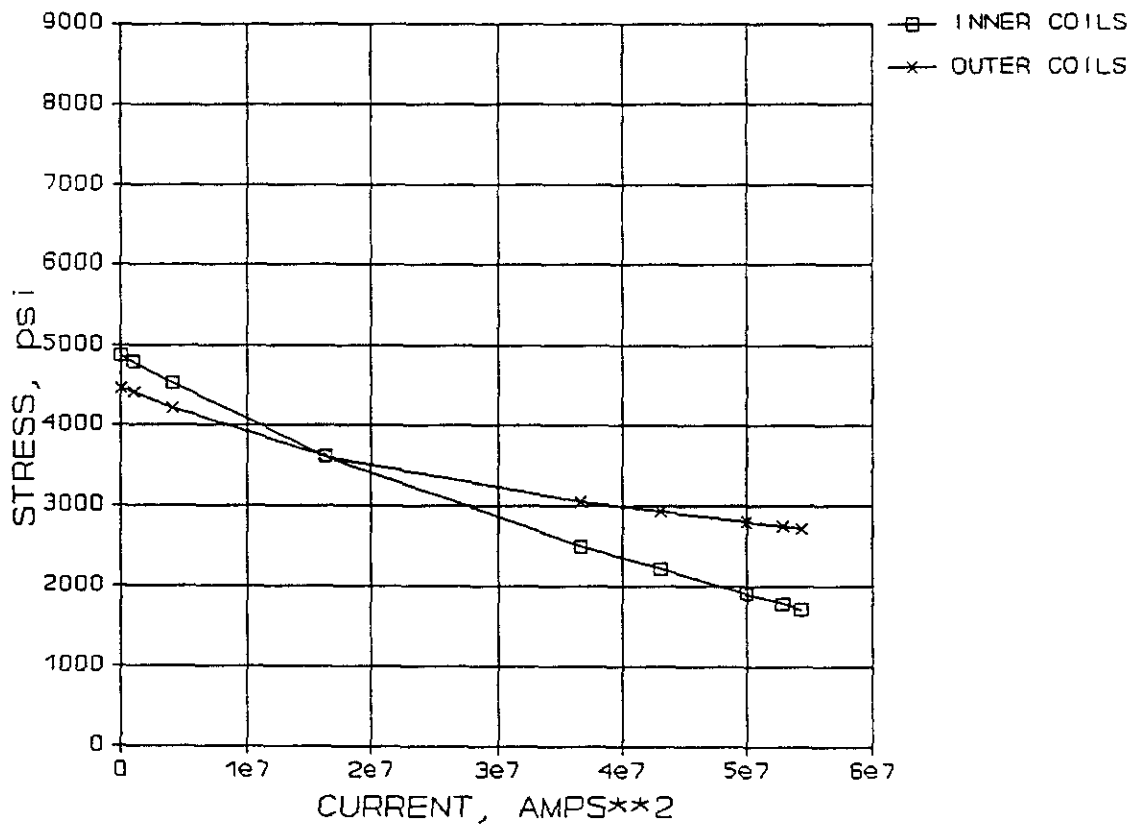
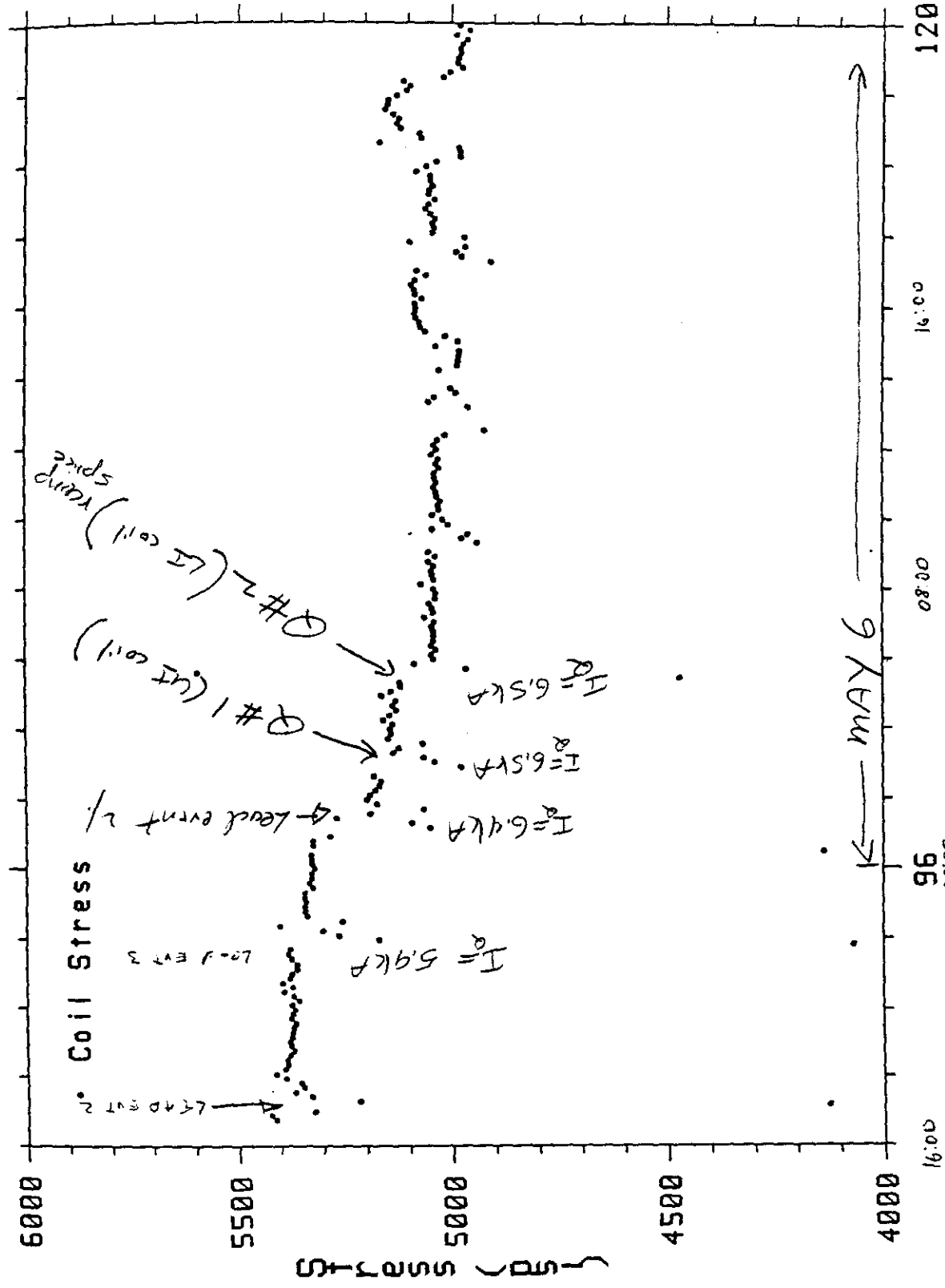


Fig. 2.II.A.2

# Average Inner Coil Stress

000012



Time (Hours since 00:00 2-May-1988)

Fig. 2.II.A.3

## B. End Plate Stress Data

The non-lead end of the magnet was instrumented with four bullet gauges, each adjusted at the time of assembly to apply 300 lbs force axially on the ends of the coils. At some stage during the work done at Fermilab, the force reading increased from 1200 lbs total to 3900 lbs total, with the four bullets continuing to track one another well. It is not known which step caused the increase. The warm history of the bullets prior to testing is shown in Fig. 2.II.B.1 (bottom).

The complete history (at zero current) is given in tabular form along with the azimuthal data in Table 2.II.A.1 (bottom). The end force increased somewhat with cooldown and during testing. The increase attributed to testing went away when the magnet was thermally cycled. There was a small increase in end force (about 100 lbs) during the initial training (time = 100 hours), as shown in Fig. 2.II.B.2.

Up to the highest current for which data are available, 7.4kA, the end force increases linearly with the square of the current (Fig. 2.II.B.1). From 0A to 6.6kA the end force increase is about 4.8 klbs, much less than the calculated value of 15 klbs. Presumably friction from the coil through the collars, shims and yoke to the skin accounts for the difference. This was advantageous in magnet operation, since experiments at BNL indicated that this class of coil end (alumina and epoxy) could fail if the end force exceeded 20 klb.

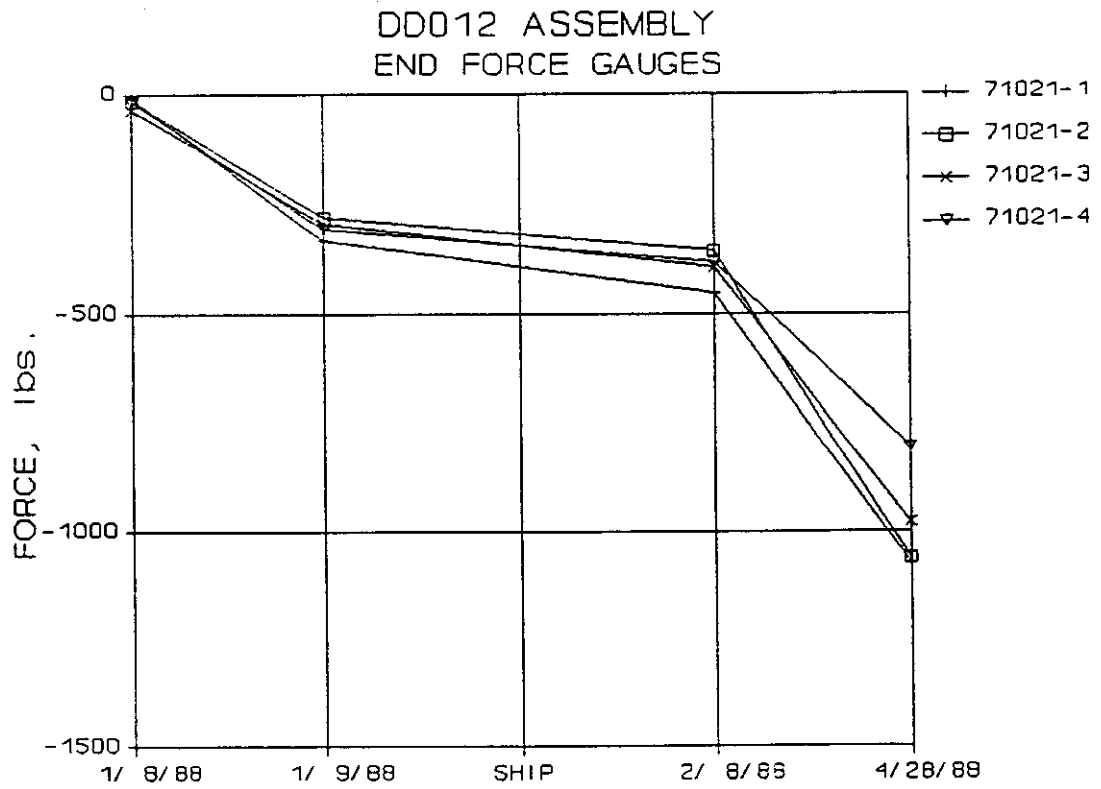
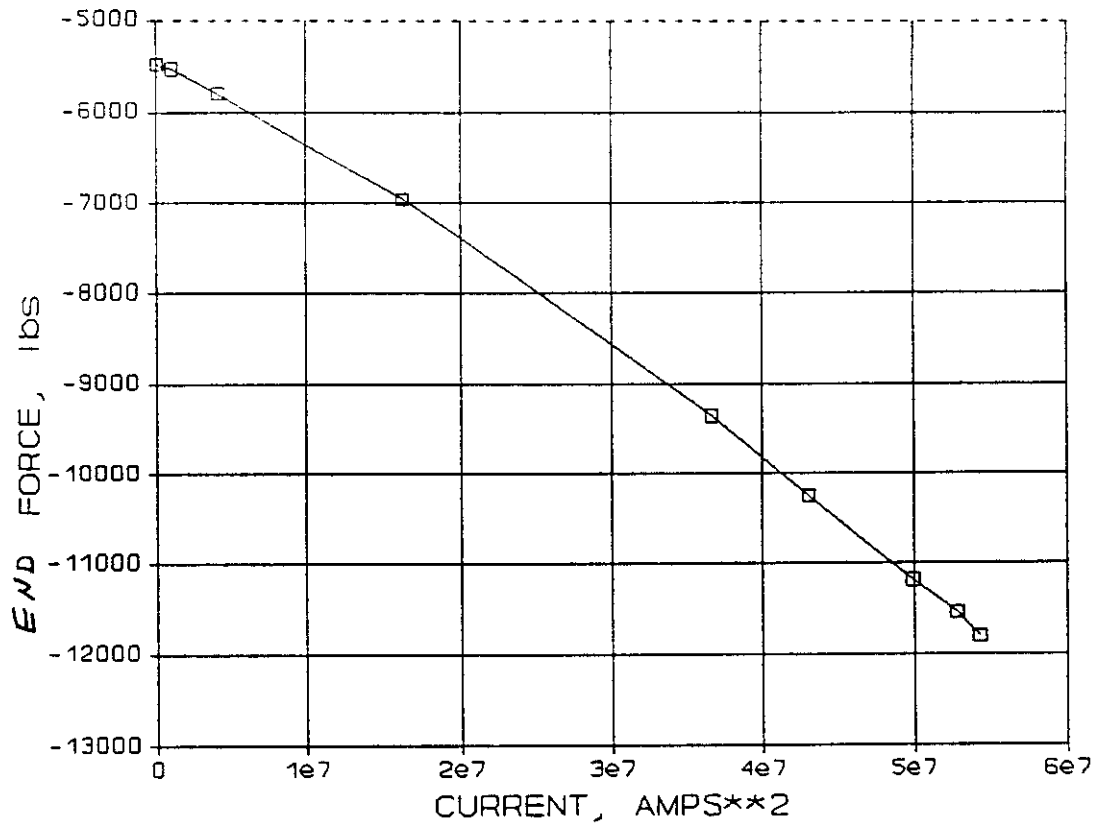
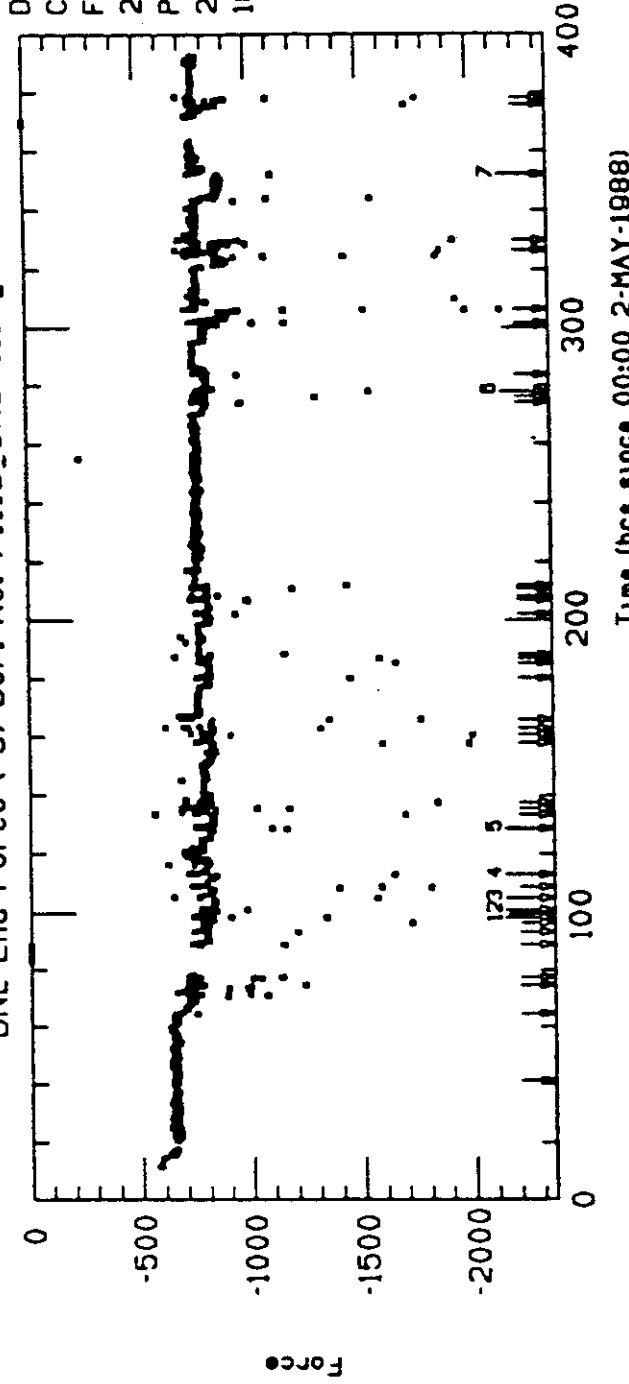


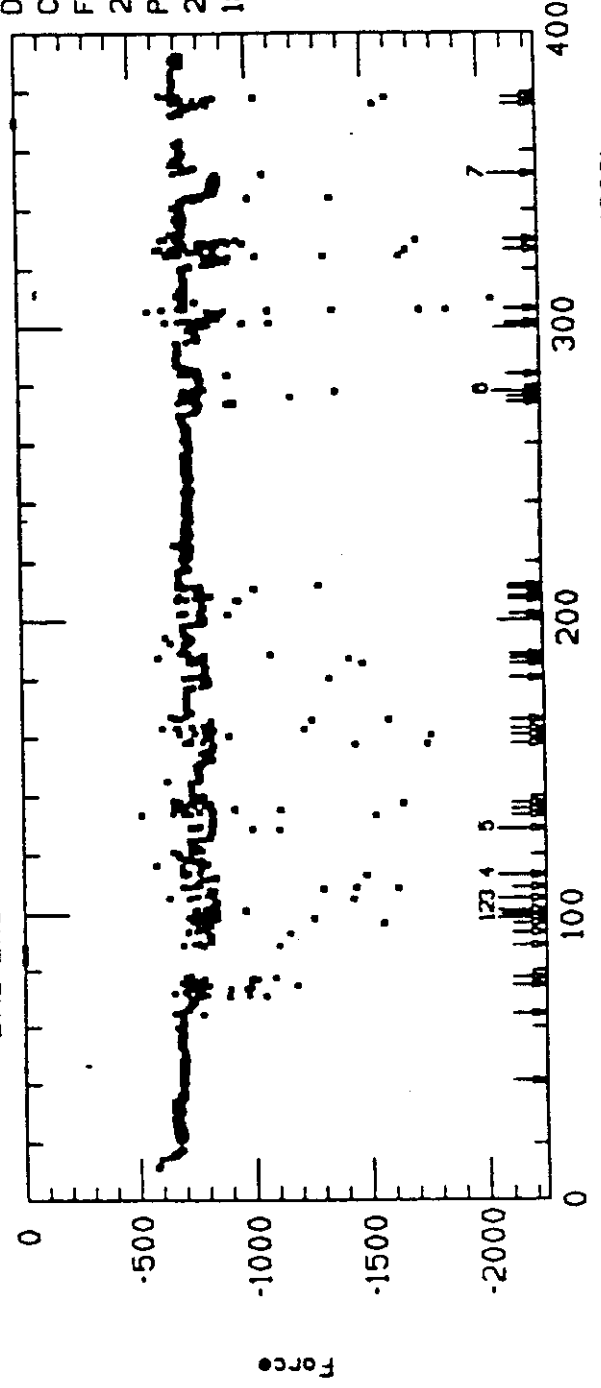
Fig. 2.II.B.1

BNL End Force ( 3) Ser. No. 71116\_3A&71116\_3B



Date File:  
CRYOLOG\_DD00012\_02.BIN  
First Data Read:  
2-MAY-1988 11:20:04  
Plot limits:  
2-MAY-1988 00:00:00  
18-MAY-1988 16:00:00

BNL End Force ( 4) Ser. No. 71116\_4A&71116\_4B



Date File:  
CRYOLOG\_DD00012\_02.BIN  
First Data Read:  
2-MAY-1988 11:20:04  
Plot limits:  
2-MAY-1988 00:00:00  
18-MAY-1988 16:00:00

Fig. 2.II.B.2

Data from the strain gauges glued to the end plates has been compared to the bullet data. The conclusion is that the results are the same, although the gauges on the end plates are less sensitive than the bullets. With this caveat, the magnet lead end behaves like the non-lead end.

### C. Cold Mass Skin Gauges

Qualitatively the data agree well with the model that the axial Lorentz force is transmitted primarily through the yoke (rather than the end plate) and is taken up by the skin within 30" of the end (Fig. 2.II.C.1). All but two of the eleven axial gauges describe a smooth variation of strain along the axis, indicating good gauge-to-gauge consistency. The response of the two azimuthal gauges was qualitatively what was expected (opposite in sign to the axial gauges; increasing response as current increased).

The gauge variation with  $I^2$  is close to linear, as expected (Fig. 2.II.C.2). However, the strain was found to vary in a stepwise fashion over many hours, for an unknown reason, making the extraction of long-term and cooldown data unreliable (Fig. 2.II.C.3). (It is thought that the problem arose because the compensating gauges were in vacuum and only weakly coupled thermally to the cold mass.) All 15 gauges had the same problem with baseline shift. Within this (large) 100 microstrain uncertainty, the shell gauges showed no dramatic changes during the course of the test.

# DD00012 Shell Strain Gages

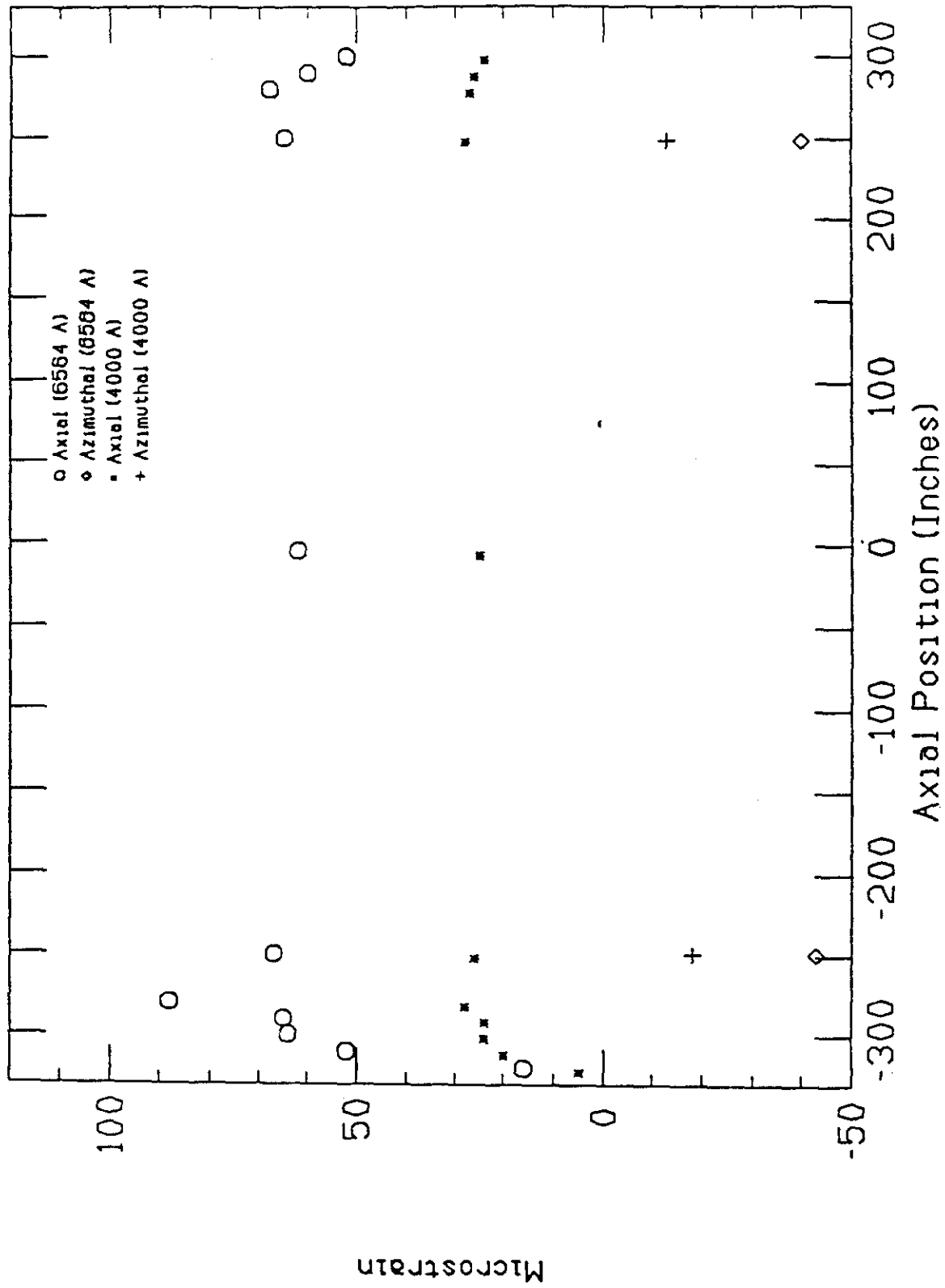


Fig. 2.II.C.1

SHELL 81" FROM FEED STRAINGAGE SG0114

SHELL 81" FROM RET STRAINGAGE SG0115

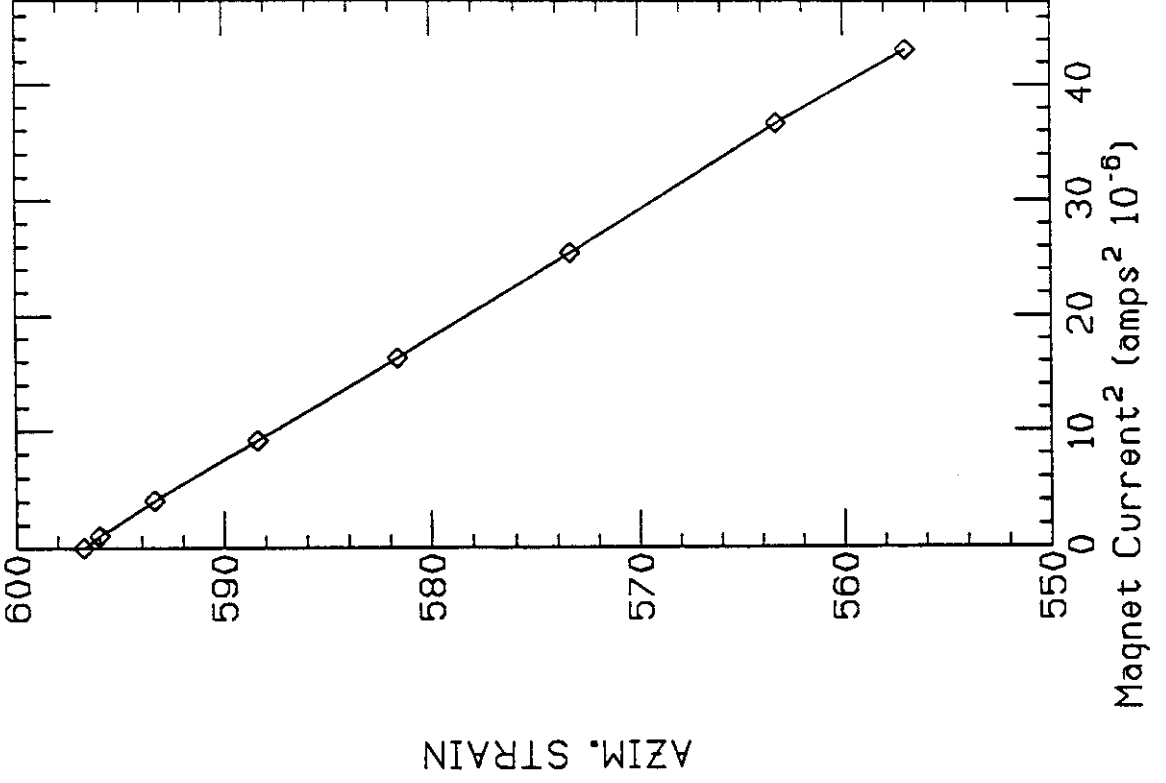
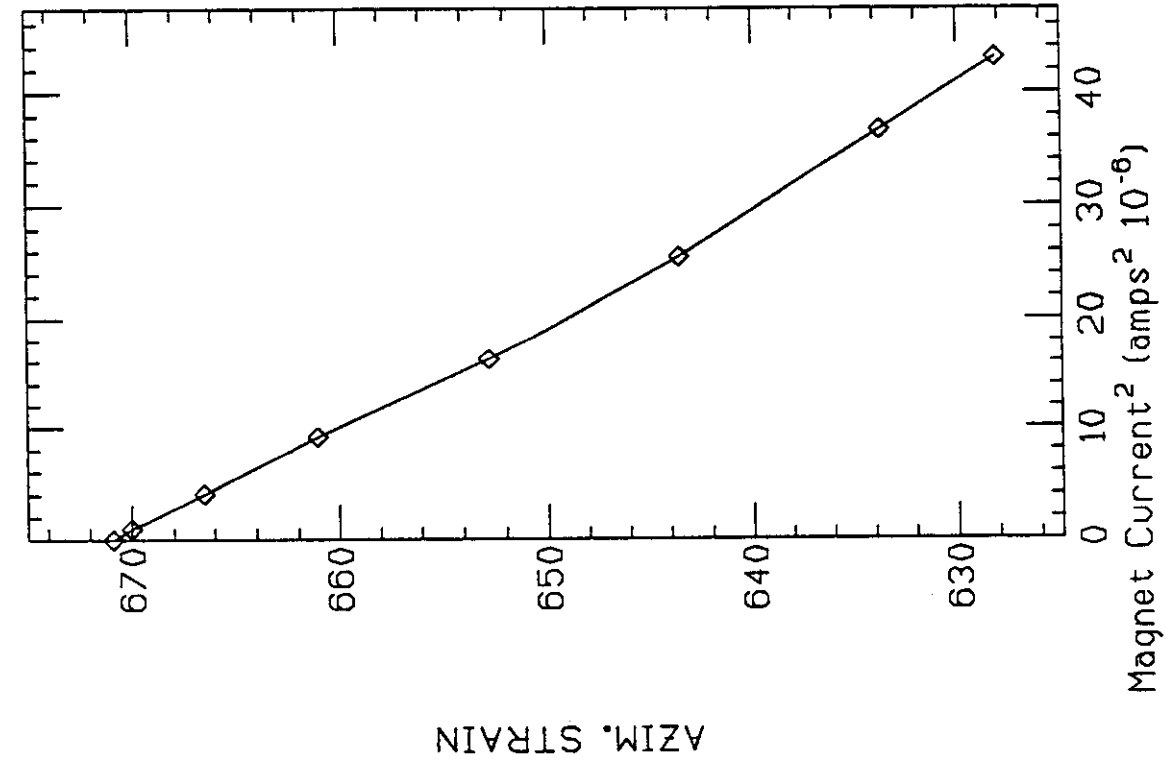


Fig. 2.II.C.2

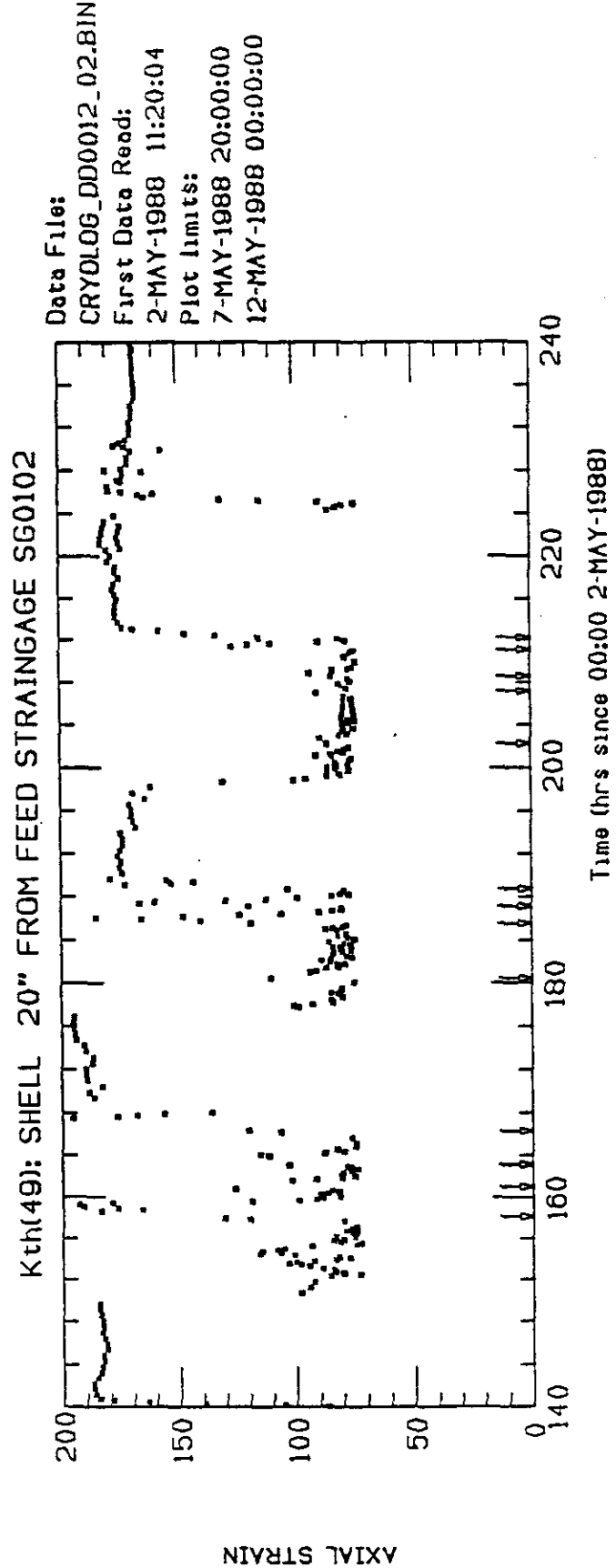
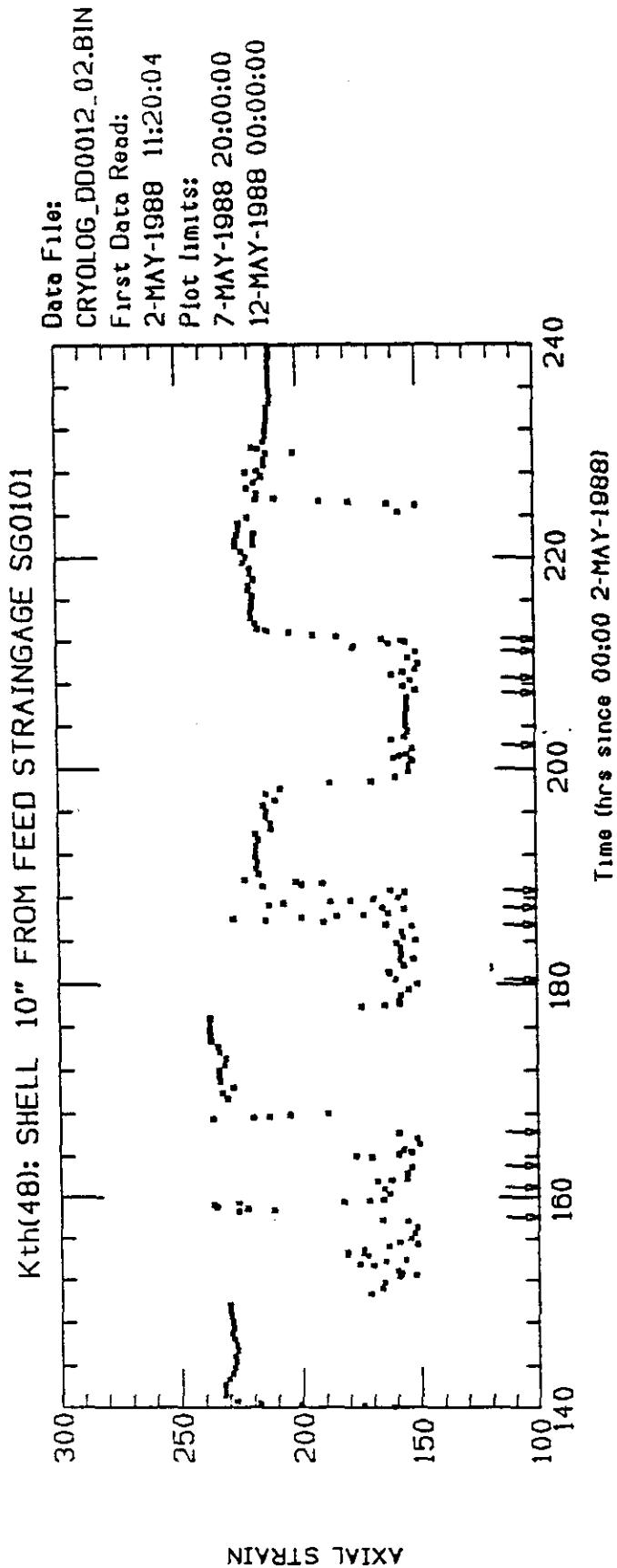


Fig. 2.II.C.3 Current equal zero and Temperature less than 4.5K.

Quantitatively, a consistent picture does not emerge, when the data are compared to calculations and other magnets. For this report, a Table of results is presented (Table 2.II.C.1). The comparison which is most free from various systematic errors is the comparison between the axial length change calculated from the eleven axial strain gauges and the same change measured by the extensometer. The same result is obtained from both, 44 mils, for excitation to 6.56 kA.

Analysis carried out at the CDG (by R. Schermer et al.) has indicated that in order to derive a complete understanding of magnet behavior, both axial and azimuthal gauges are needed. It has also been recommended that strain gauge rosettes be used in the future rebuild of this magnet.

#### D. Extensometer

The data for cooldown indicate that the magnet shrinks 100 mils more than the stainless steel rod on which the extensometer is mounted. This is a surprise, since the thermal contraction of the rod and skin are expected to be nearly identical and the collared coil is expected to resist the contraction of the skin. Also, the extensometer cooldown data are at variance with the axial skin strain gauge data.

The plot of extensometer with time shows that the (cold) magnet became longer by 2 mils at the time of the second lead event (Fig. 2.II.D.1). After correction for backlash, the extensometer also shows that the magnet lengthens linearly with  $I^2$  to a total of 44 mils at 6.56 kA (Fig. 2.II.D.2).

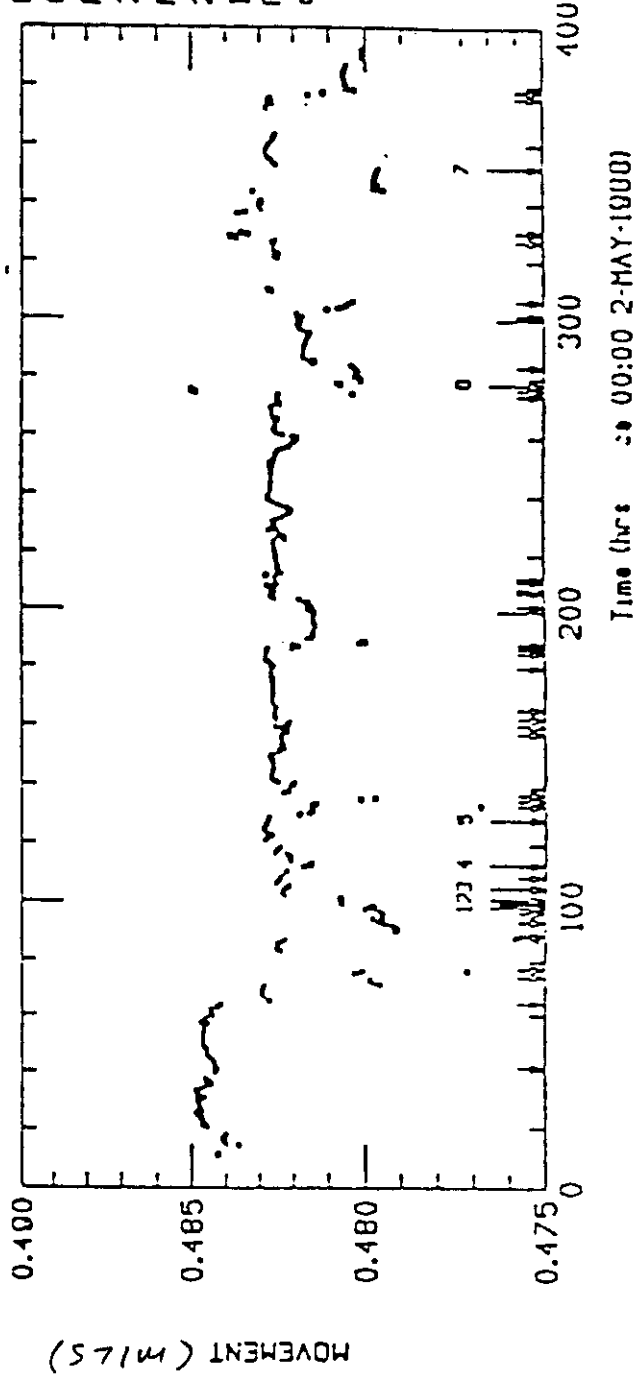
Table I. STRAIN, STRESS AND LENGTH CHANGE OF MAGNET SHELLS

MAGNET	STATE	-----MEASURED-----				---CALCULATED---		
		$\Delta L$ (in)	$\Delta(\epsilon_{\theta} - \alpha\Delta T)$ ( $\mu\epsilon$ )	$\Delta(\epsilon_z - \alpha\Delta T)$ ( $\mu\epsilon$ )	$\Delta\sigma_{\theta}$ (psi)	$\Delta\sigma_z$ (psi)	$\Delta\sigma_{\theta}$ (psi)	$\Delta\sigma_z$ (psi)
DSS6A	COOLDOWN	-----	+430 <sup>1</sup>	-79 <sup>2</sup>	13400	+1660		
	6.4 KA	-----	-25 <sup>1</sup>	+23 <sup>2</sup>	-610	+510		
DD0010	COOLDOWN <sup>4</sup>	-2.044 <sup>6</sup>	+710 <sup>3</sup>	+100	+24400	+10300		
	COOLDOWN <sup>5</sup>		+16		+23600	+7550		
	5.05 KA	+0.020	-12 <sup>3</sup>	+38 <sup>7</sup>	-20	+1130		
DD0012	COOLDOWN <sup>4</sup>	-0.10 <sup>8</sup>	+630 <sup>3</sup>	+230	+25700	+14600	<i>all axial gages</i>	
	COOLDOWN <sup>5</sup>	+0.044	-42 <sup>3</sup>	-150	+21900	+2080	<i>b.z.</i>	
	6.56 KA	<i>67 <math>\mu\epsilon</math> axially</i>	<i>42</i>	<i>2310 psi</i>	-690	+1900		
			<i>x33</i>					
			<i>-1386 psi</i>					

1. Average of azimuthal gages 2 and 3.
2. Average of all 4 axial gages.
3. Average of both azimuthal gages.
4. Axial strain computed from average of all axial gages.
5. Axial strain computed from  $\Delta L$ .
6. Shell contraction relative to quartz, corrected for sensor nonlinearity.
7. Average of axial gages in central section only.
8. Shell contraction relative to 304 stainless steel.

10 JUN 88 12:24:53

Ktlh(76): COLD MASS SHELL EXTENSIOINT EXT-01  
CALIBRATION ADJUSTED FOR 2 INCH SENSOR



Date File (last if >1):  
CRYOLOG\_DD0012\_02.DIN  
First Date Read:  
2-MAY-1988 11:20:04  
Plot limits:  
2-MAY-1988 00:00:00  
18-MAY-1988 10:00:00  
For magnet current < 10.0 amp  
and temperature < 5.000 K

Fig. 2.II.D.1

DD0012: COLD MASS SHELL EXTENSION EXT-01  
CALIBRATION ADJUSTED FOR 2 INCH SENSOR

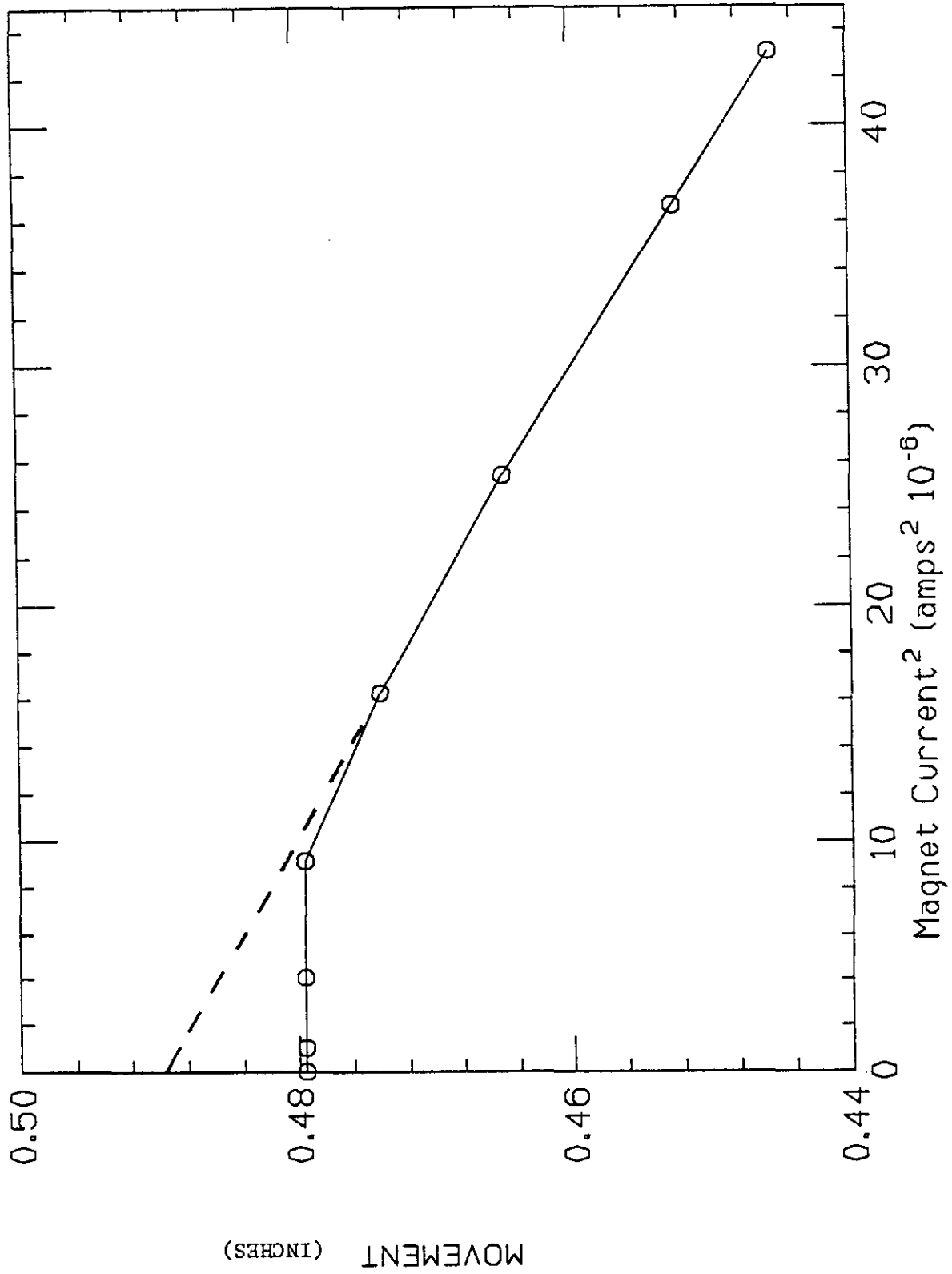


Fig. 2.II.D.2

Schermer (at the Aug MSIM) concluded that the extensometer data are redundant with respect to the skin axial gauges. He also concluded that it was easier to interpret data from a stainless steel rod than from a quartz rod.

#### E. End plate motion transducer (Niemann gauge)

Schermer concluded that these gauges are not useful for magnets with thick end plates, because the end plate motion is so small. The early time history (Fig. 2.II.E.1) shows a change of 1 microstrain during the initial few quenches. A signal of about 3 microstrain can be seen during the excitation to 5.5kA (Fig. 2.II.E.2).

### III. Quench Behavior.

#### A. Quench Currents

The quench history of this magnet is given in Fig. 2-III-A-1. The first quench (6520A) was at the limit of the conductor. The current was 2% higher than a calculation based on the measured short-sample result, extrapolated to operation in the magnet at 4.4K (6.38 kA). The difference between these values is typical of this cable. (Cable from the same billets was used in the 1.8m dipoles DSS10-12.)

A detailed comparison of magnet quench current and temperature is made in Fig. 2-III-A-2. Most of the quenches originated near the feed or return ends of the magnet. Using the temperatures from the corresponding feed can and return can

27-MAY-00 14:14:12

KUNIGI: END PLATE (FEED) STRAINGAGE SG0110 /D025

Date File:  
CRYLOG\_D00012\_02.DIN  
First Date Read:  
2-MAY-1000 11:20:04  
Plot limits:  
2-MAY-1000 00:00:00  
10-MAY-1000 10:00:00

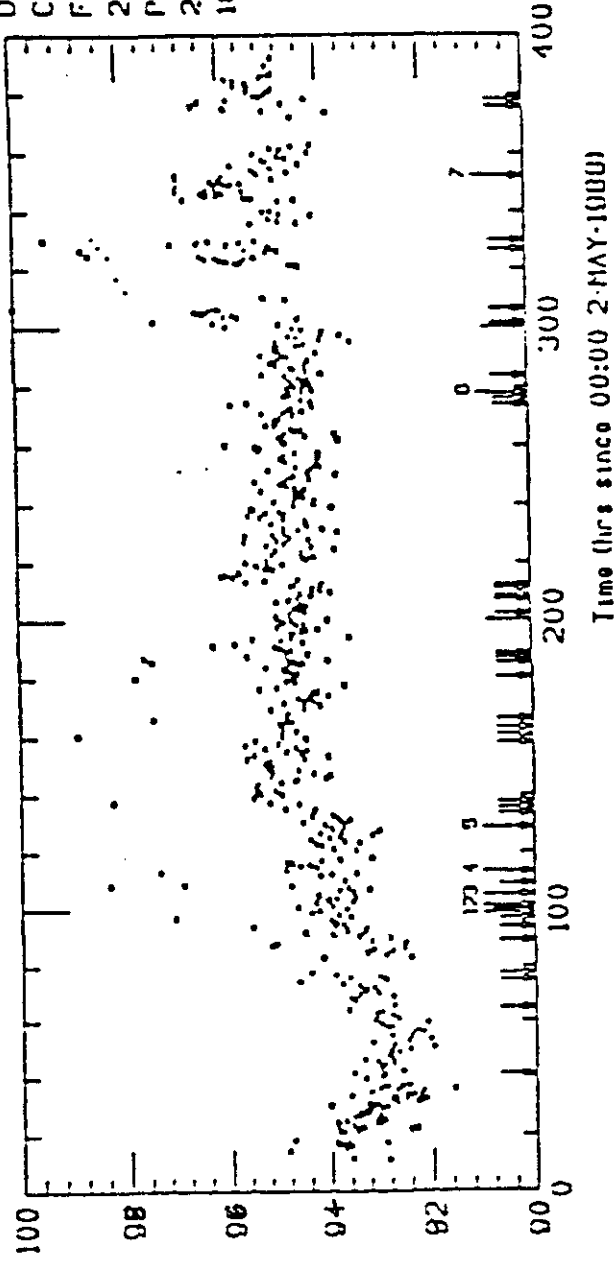


Fig. 2.II.E.1

# Lead End Motion

DD0012

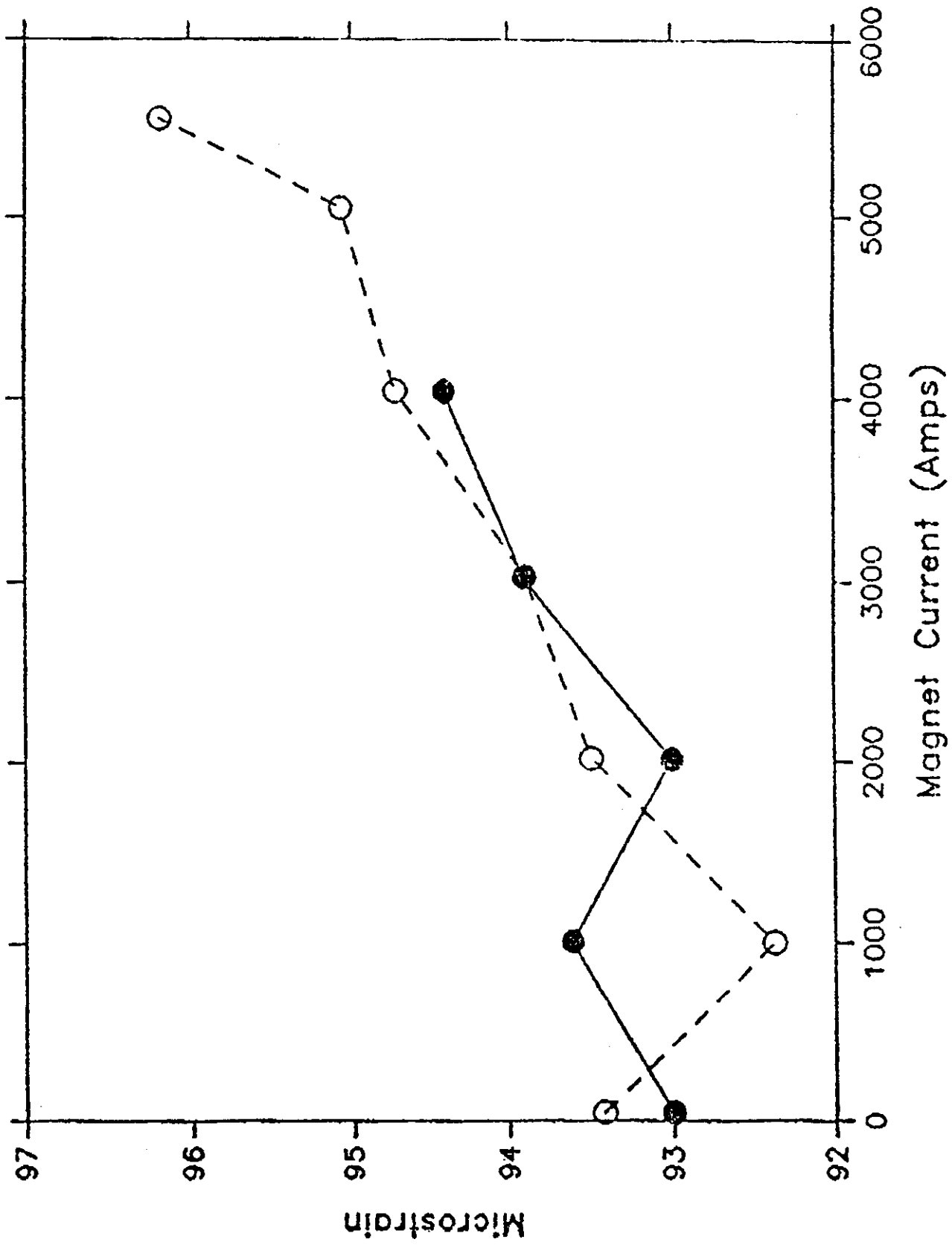


Fig. 2.II.E.2

DD12 Current at Quench

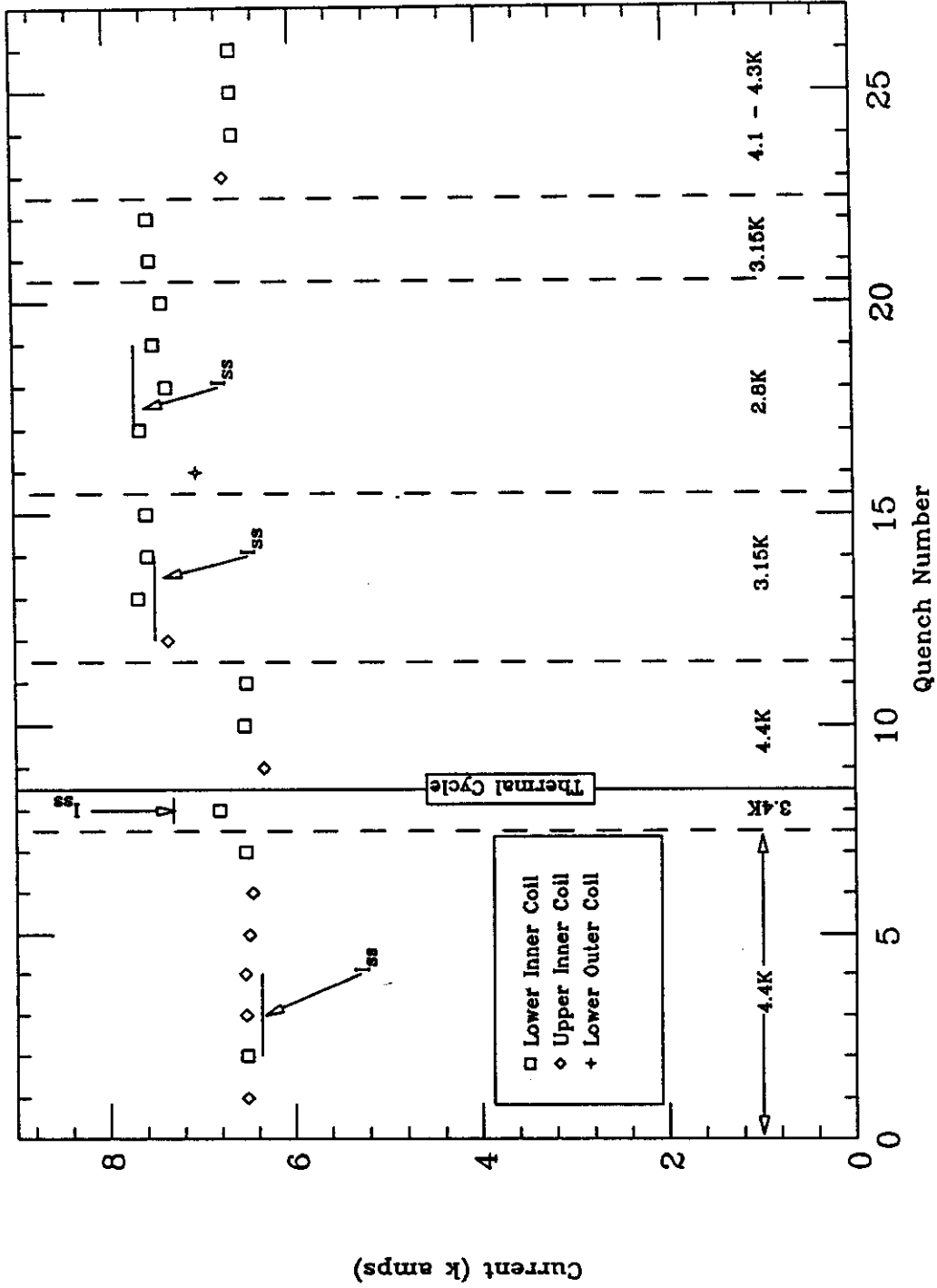


Fig. 2.III.A.1

$I_{SS}$  from SSC-N-519

### DD0012: Quench Current vs. Temperature

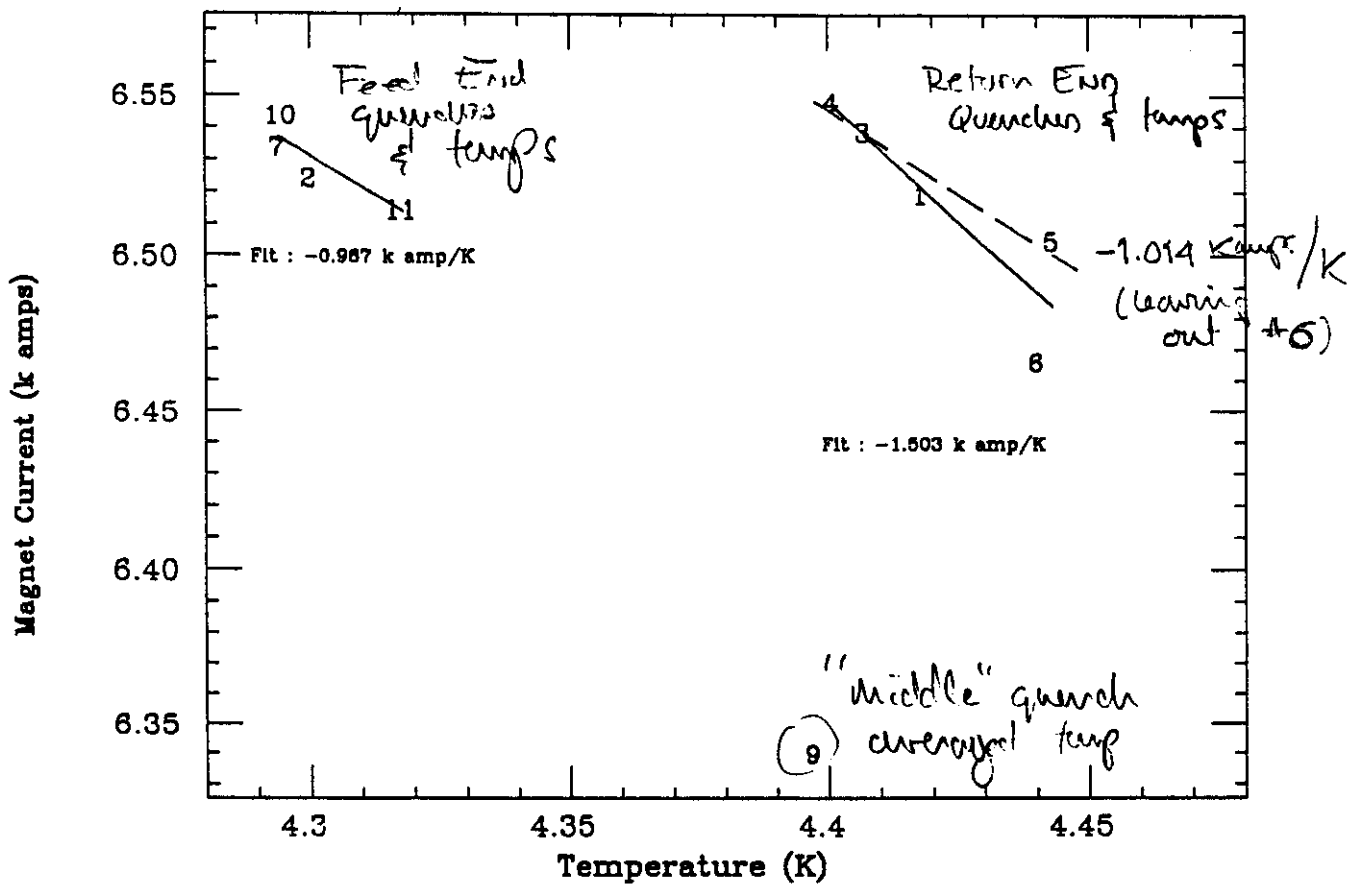


Fig. 2.III.A.2

thermometers yields the expected linear relations between temperature and quench current, with scatter at the 10A level. The fits to the data are close to the value calculated with Morgan's parameterization, which lies in the range 1.06 - 1.09 kA/K at this temperature. (Two quenches do not fit this pattern. Quench 9 is a retraining quench after the thermal cycle. Quench 6 occurred after the magnet had been held at a fixed current for 15 sec prior to a spot heater quench, rather than during the usual 16A/sec ramp.) The highest quench current was 7675A (quench 13). The magnet was thermally cycled between quenches 8 and 9 in coincidence with a warmup for cleaning out the refrigerator purifiers.

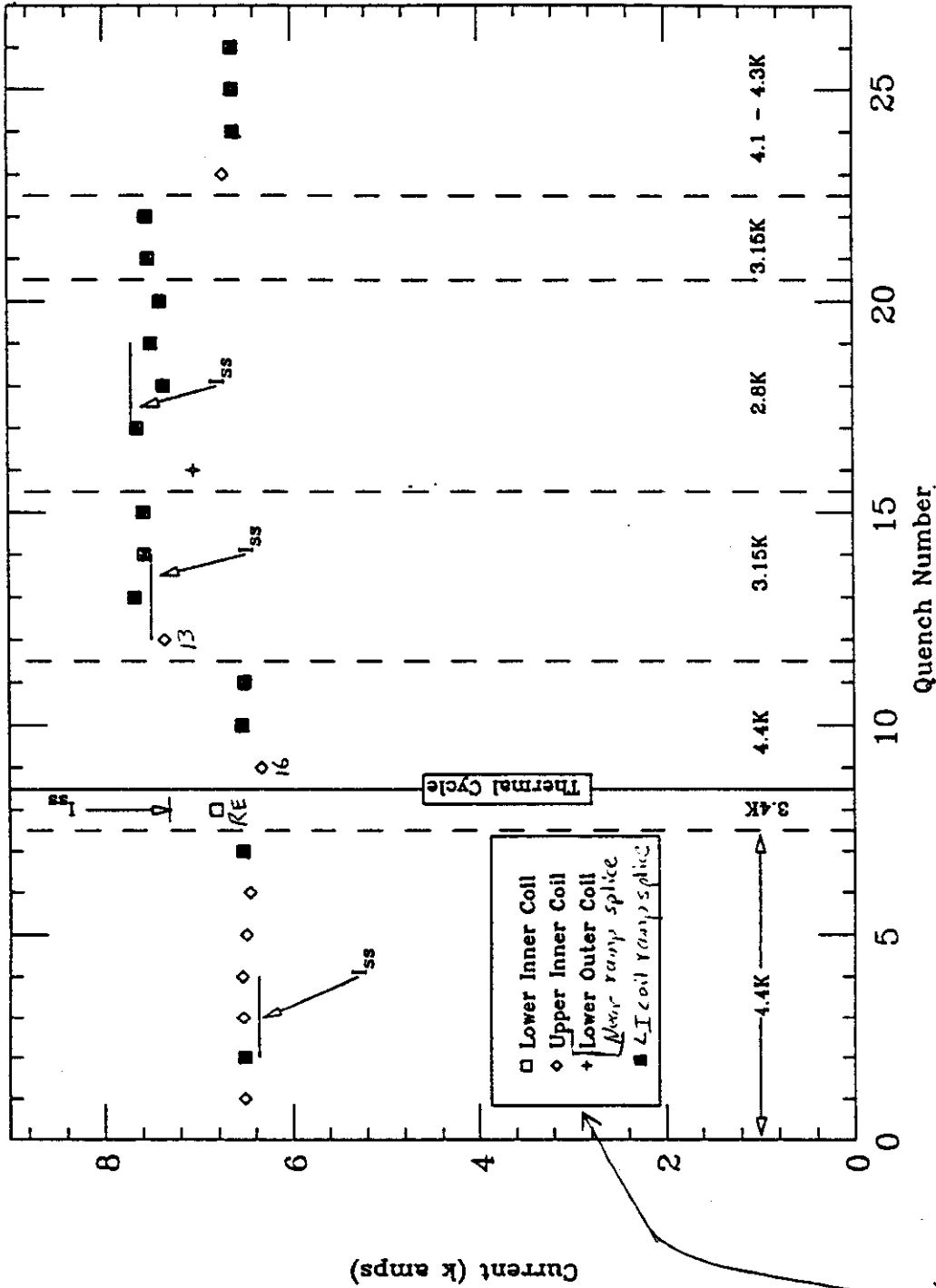
#### B. Quench Location

The quench locations have been summarized in an annotated version of the quench plot, Fig. 2-III-B-1. It can be seen that the magnet plateau quenches at 4.4K originated in the expected location, the two-dimensional peak-field (in the straight section of inner coil turn 16, which is nearest the pole). At the lowest temperature, 2.8K, the magnet performance was limited by quenches originating in the ramp-slice. The same limitation probably also applied at 3.15K.

The four training quenches originated in inner coil turns 13 (next to the largest wedge) and 16 (straight-section and return end). The outer coil quench originated near the splice.

#### C. Associated Data (Spot heaters, MIITS, Propagation Velocities)

DD12 Current at Quench and Quench Origin Summary



◇ Plateau quenches (UI coil, Return End, at voltage top)  $I_{ss}$  from SSC-N-519  
 ◇<sub>n</sub> - straight section quenches; n = turn number  
 RE - return end

Fig. 2.III.B.1

The average longitudinal velocity was calculated from the coil length and the time it took for the quench to propagate from the origin to both of the ends. Representative data for spontaneous quenches are shown in Figs. 2.III.C.1 and .2. The first of these figures gives results for five quenches of nearly identical currents, the limit of the conductor at 4.4K. These quenches originated in the magnet straight-section, at the voltage tap which marks the "beginning" of the end region but is actually about 17.5" into the magnet straight section from the return end. The turn where the quench originates, turn 16, is the turn nearest the pole. Longitudinal velocities of quenches at the same temperature but originating in the ramp-splice are quite similar. The next figure (2.III.C.2) shows the velocity at higher current and lower temperature. The quenches originated in the ramp-splice and were near but not at the plateau current for this temperature.

Further data on the variation of quench velocity with magnet current are given in Figs. 2.III.C.3 and .4, which show velocities as a function of turn number for quenches produced by spot heaters 9" and 48" into the straight section of the midplane turn (turn 1). The magnet currents were 88% and 99% of the quench plateau (4.4K).

The azimuthal velocity, given as the turn-to-turn propagation time (Figs. 2-III-C-5 and -6) varies from 1 ms to 7ms for spontaneous quenches at 4.4K. It shows a similarly strong variation for spot-heater induced quenches (Figs. 2.III.C.7 and .8). These variations are not understood at the

### Longitudinal velocity vs. Number of turn

(DD0012 - Avg. velocity for quenches 1,3-6)

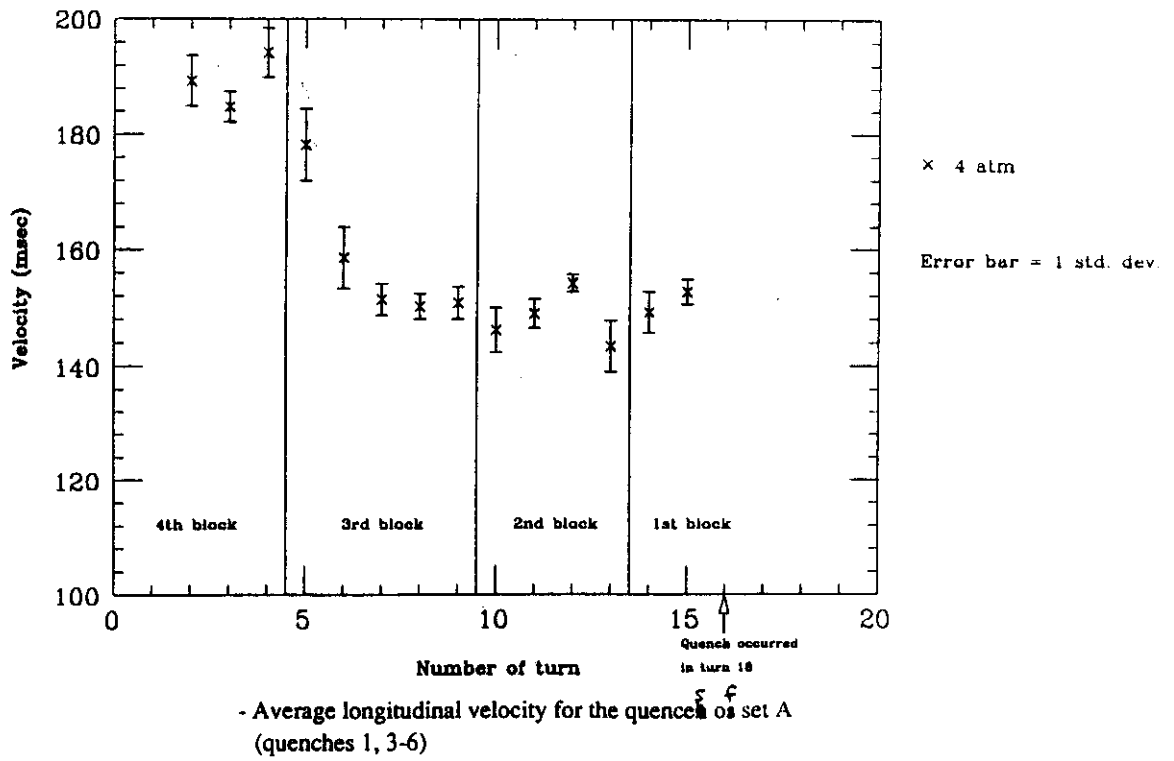


Fig. 2.III.C.1

### Longitudinal velocity vs. Number of turn

(DD0012 - Ramp splice quenches at 3.1K)

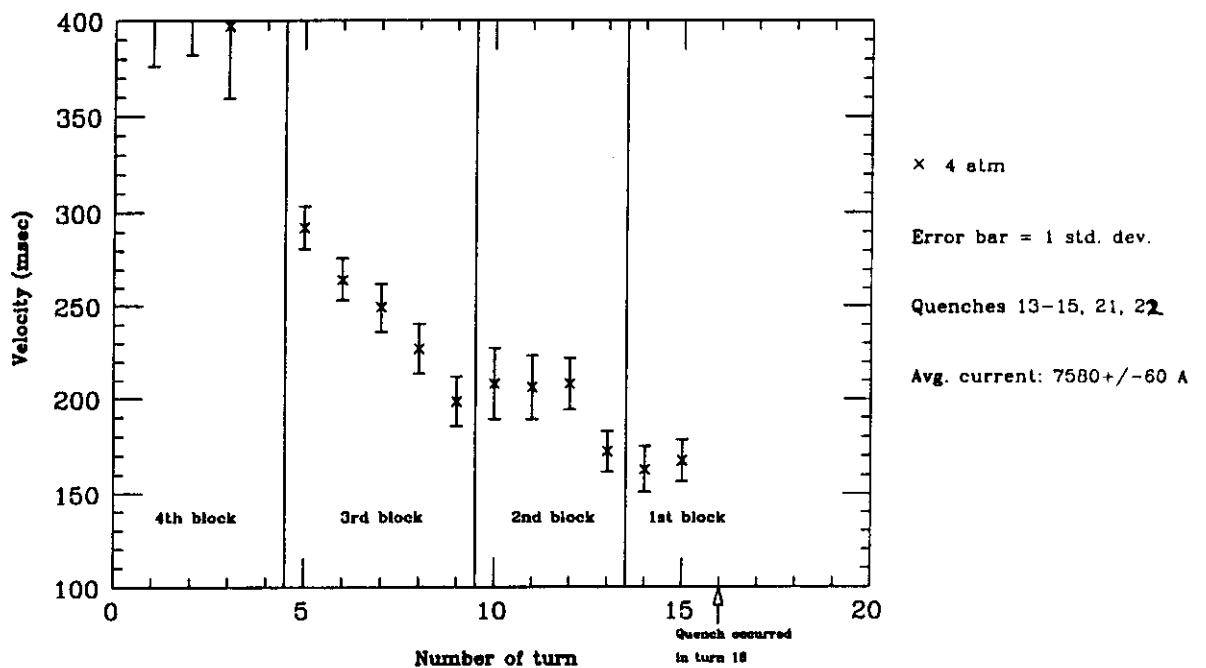


Fig. 2.III.C.2  
Average longitudinal quench propagation velocity for the five ramp splice quenches at 3 K.

### Avg. velocity vs. Number of turn

For spot heater runs at 5753 A

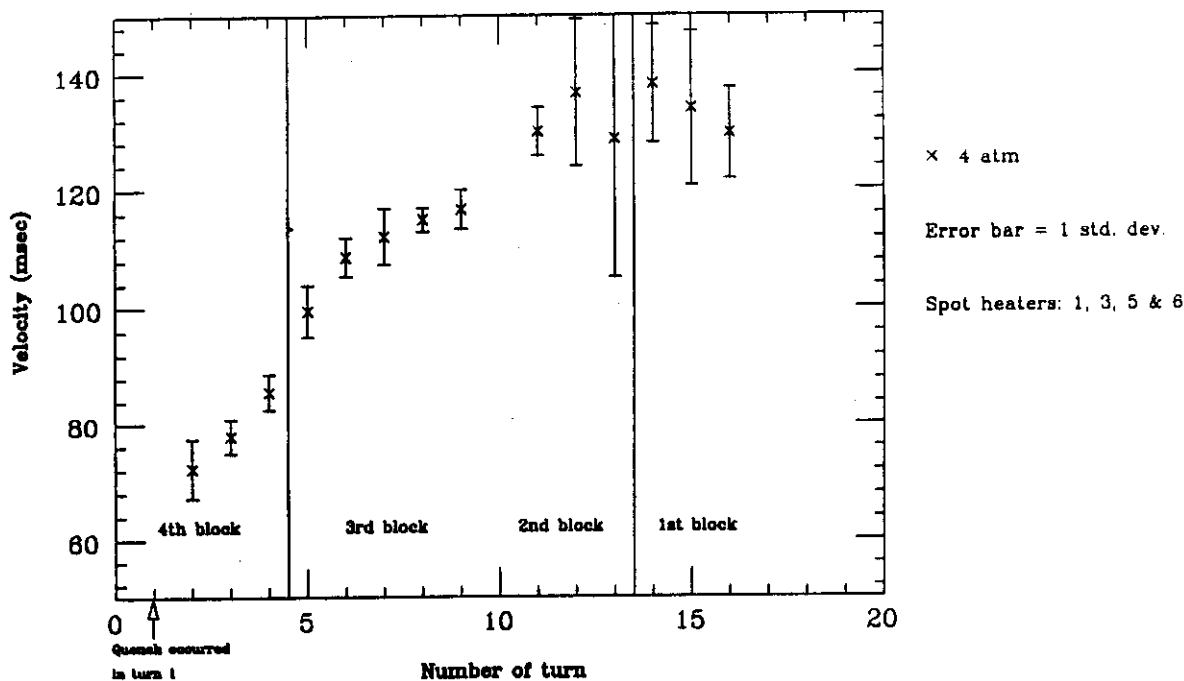


Fig. 2.III.C.3

Average longitudinal velocity plot for each quench at 5753 A.

### Avg. velocity vs. Number of turn

For spot heater runs at 6466 A

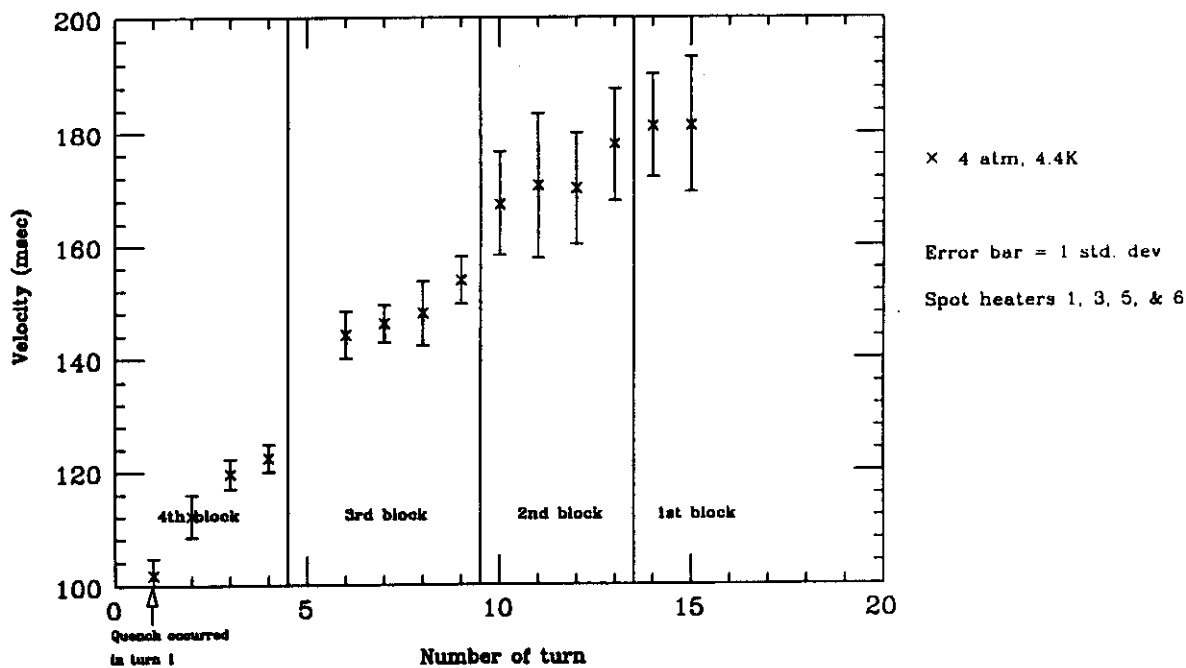


Fig. 2.III.C.4

Average longitudinal velocity plot for each quench at 6466 A.

### Transversal Time vs. Number of turn

(DD0012 - Avg. time for quenches 1,3-6)

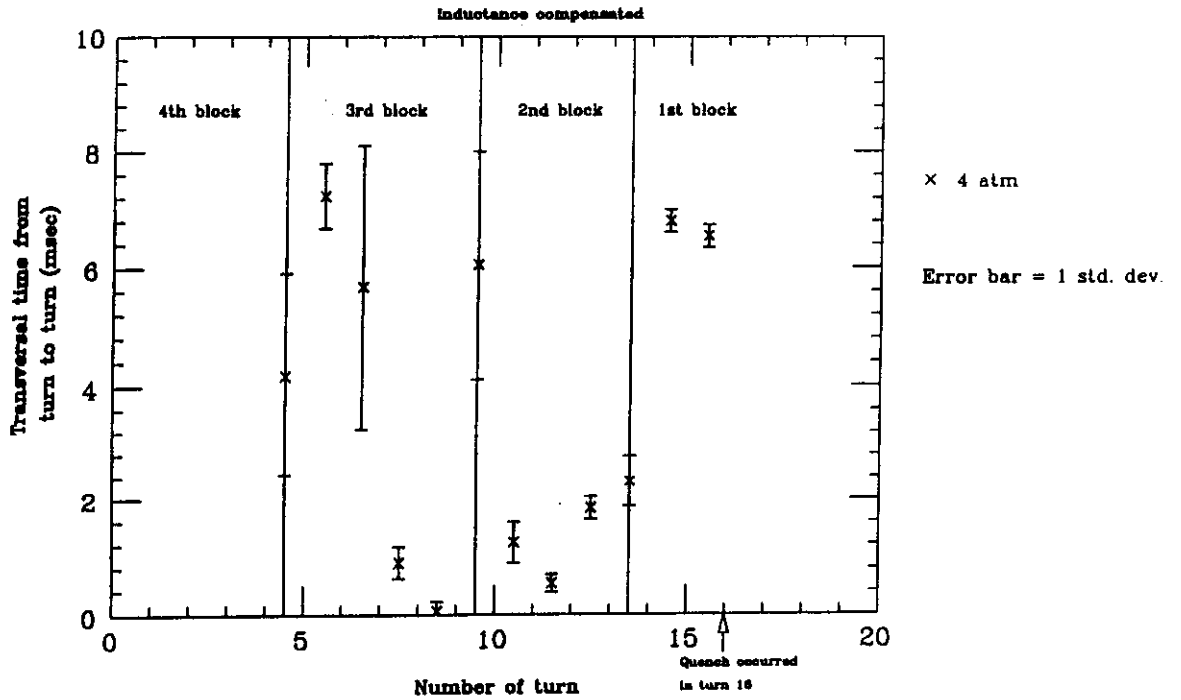


Fig. 2.III.C.5

Average transversal propagation time for all the quenches of Set A

### Transversal Time vs. Number of turn

(DD0012 - Avg time, quenches 7,10,11,24-28)

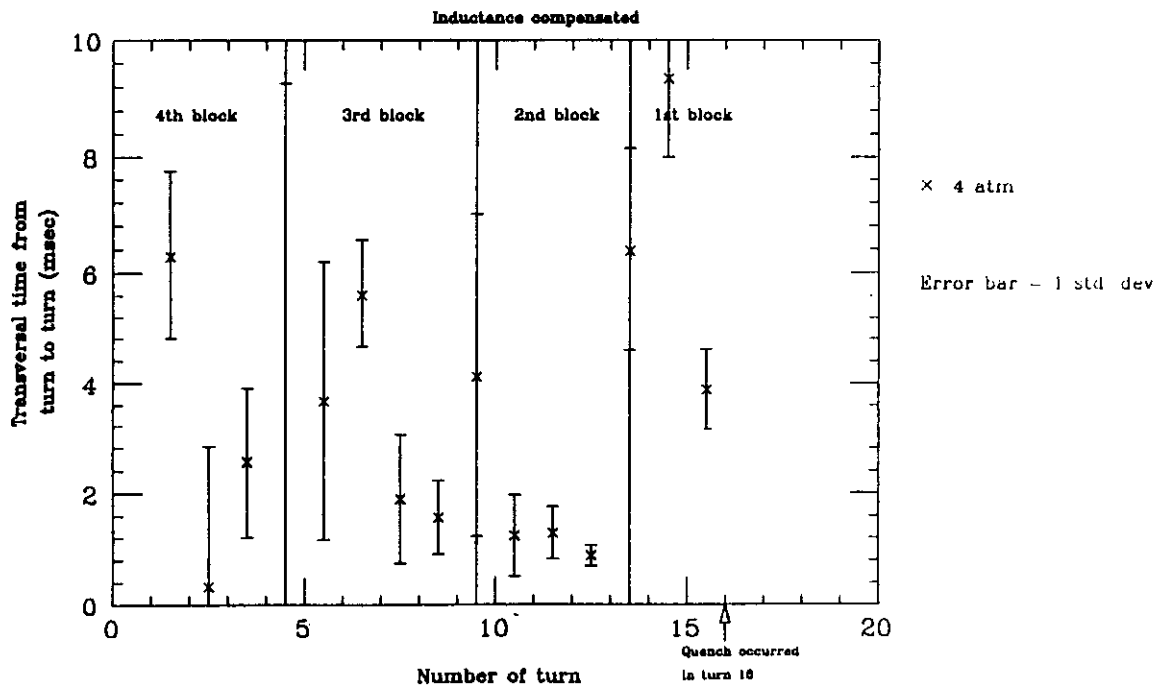
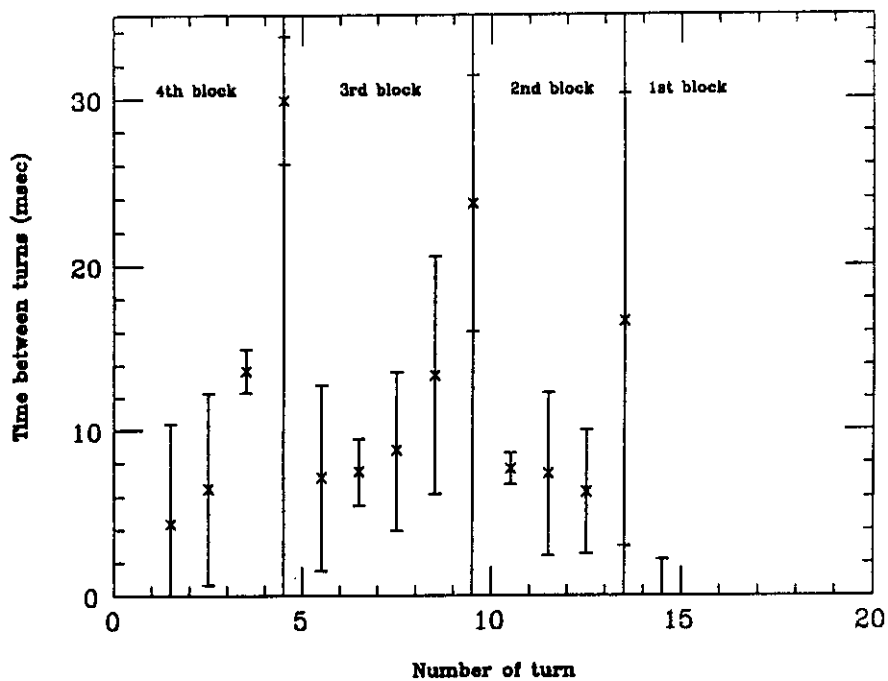


Fig. 2. III.C.6

Average transversal propagation time for all the quenches of Set B

### Avg. Transversal Time vs. Number of turn

(DD0012 - I = 5753 A - 4.4 K)



x 4 atm I=5753 A

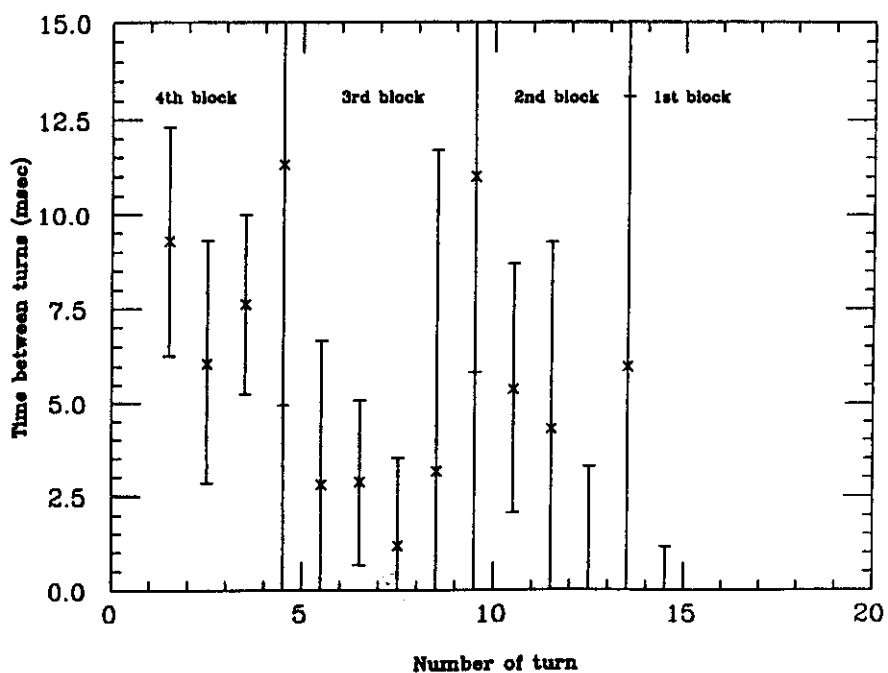
Avg. of spot heaters  
1, 3, 5, & 8

Fig. 2.III.C.7

Average transverse time for all quenches at 5753 A.

### Avg. Transversal Time vs. Number of turn

(DD0012 - I = 6466 A - 4.4 K)



x 4 atm I=6466 A

Avg. of spot heaters  
1, 3, 5, & 8

Fig. 2.III.C.8

Average transverse time for all quenches at 6466 A.

present time. (Quench velocity data are from analyses by Devred and Cortella, SSC informal notes MD-TA-90, 91, 92.)

At 4.4K, the plateau quenches had typical MIITS values of 8.1 with the standard 130ms strip heater delay. At the same temperature, at a current of 5.8kA, the MIITS produced by the four spot heaters ranged from 10.3 to 10.8. At 3.0kA, the MIITS increased from 5.85 to 10.42 when the strip heater delay was increased to 480ms (i.e., making essentially no use of the heaters). At 2.8K, the maximum MIITS was 10.4. (MIITS values are from Tompkins' program.)

#### IV. Summary of Test Results.

At SSC operating temperature, the magnet needed no training to reach the limit of the conductor, 6.52 kA (6.6T). After a thermal cycle, the magnet quenched once at 6.34 kA before again reaching the conductor limit. Some training was needed to reach quench currents in the range 7.5 kA at lower temperature. These quenches originated in the ramp-splice. The longitudinal velocities of the plateau quenches at 4.4K are 150 m/s. Turn-to-turn propagation times range from 1 ms to 7 ms.

The new beam-type azimuthal strain gauges in the coils seemed to be working as designed and indicated that there was finite prestress left at the highest currents tested, 7.4kA (about 7.4T). However, the overall scale of the axial forces was smaller than expected. The axial Lorentz force was taken

up within 30 inches of the end of the yoke skin. Data from the skin are not entirely consistent with calculations. The effects of the initial few quenches can be seen in the strain gauge data, but are small.

## V. Exceptions During Testing

### A. Rapid quench propagation in non-quenching winding.

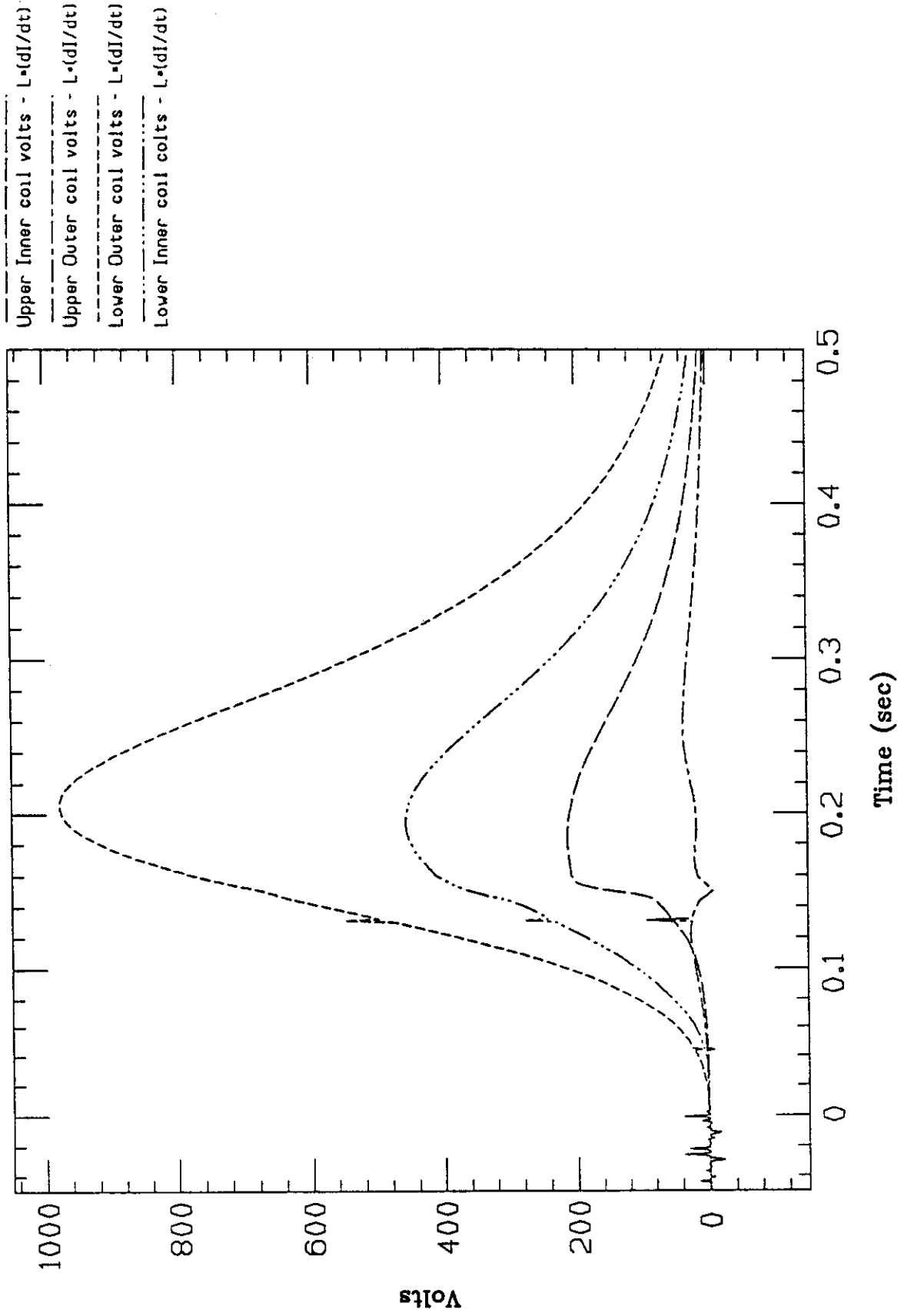
For a quench originating in the lower outer winding, each turn in the upper inner winding experienced a sudden increase in voltage during a 10 ms period about 150 ms after the quench was detected. Various traces from this quench (number 16) are shown in Figs. 2-V-A-1 through -5. The voltage increase is presumed to be due to an increase in coil resistance, a result of an unusual mechanism for quench propagation.

A similar event was found in quench 13. In this case, the quench originated in the lower inner coil. The rapid increase in voltage was seen in both the lower inner and the upper inner coil about 95 ms after the quench was detected (Figs. 2-V-A-6 and -7). Less of a jump was seen in another quench (quench 4, Figs. -8 and -9).

### B. Unusual behavior of magnet current following spot heater quench.

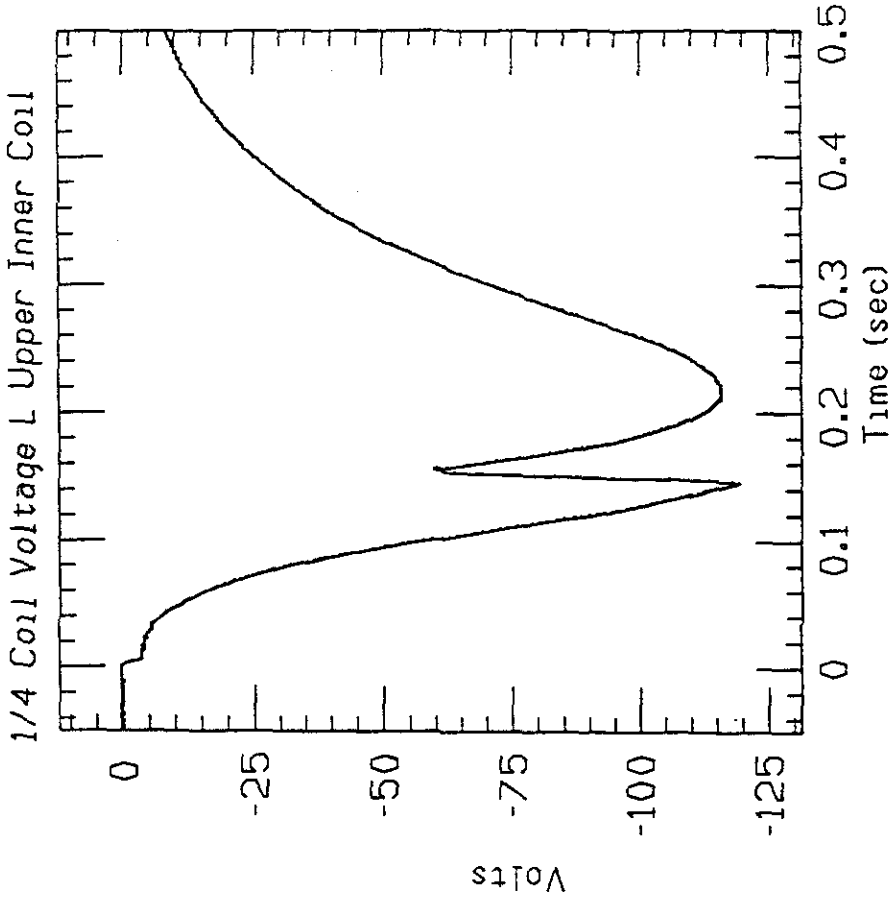
An irregularity was found in the current trace after a spot heater quench (file 91), as indicated in Fig. 2-V-B-1. The irregularity was seen in both the transducer and the shunt

### DD0012: Resistive Voltage - Quarter Coils

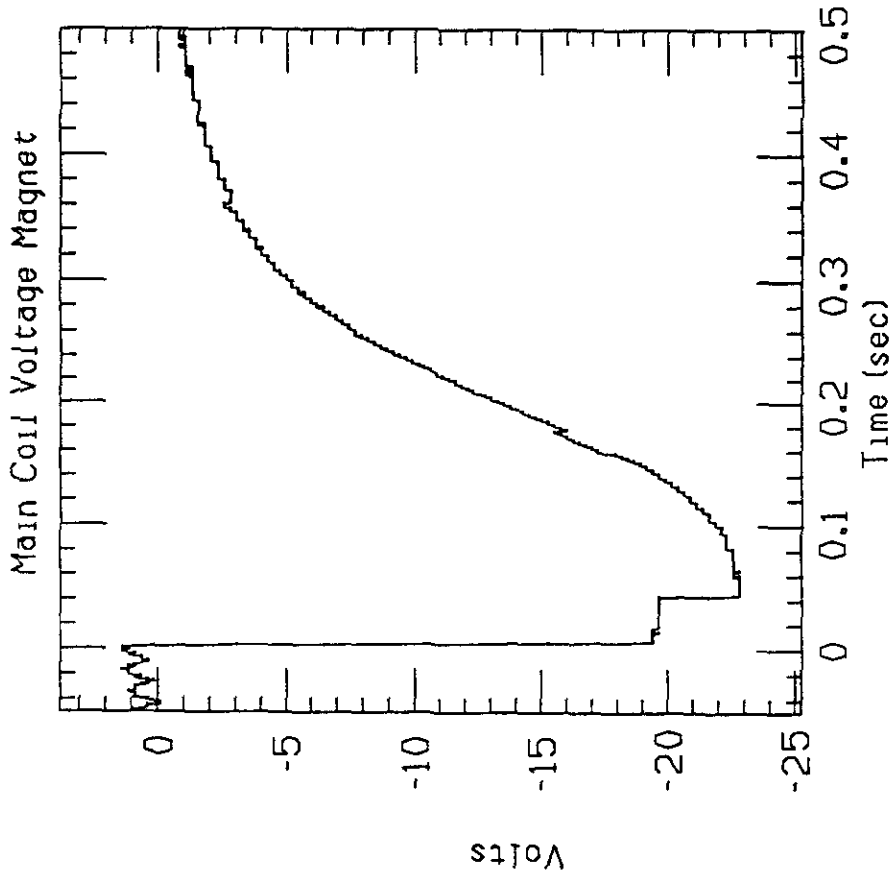


File : DD0012.QB082 Magnet : DD0012 - Quench Date : 24-JUN-88 - 06:02:14 Quench # 16  
S.C.# 1 I(quench) = 7050.6 (amps) MIITs = 10.055 TO = -0.014

Fig. 2.V.A.1

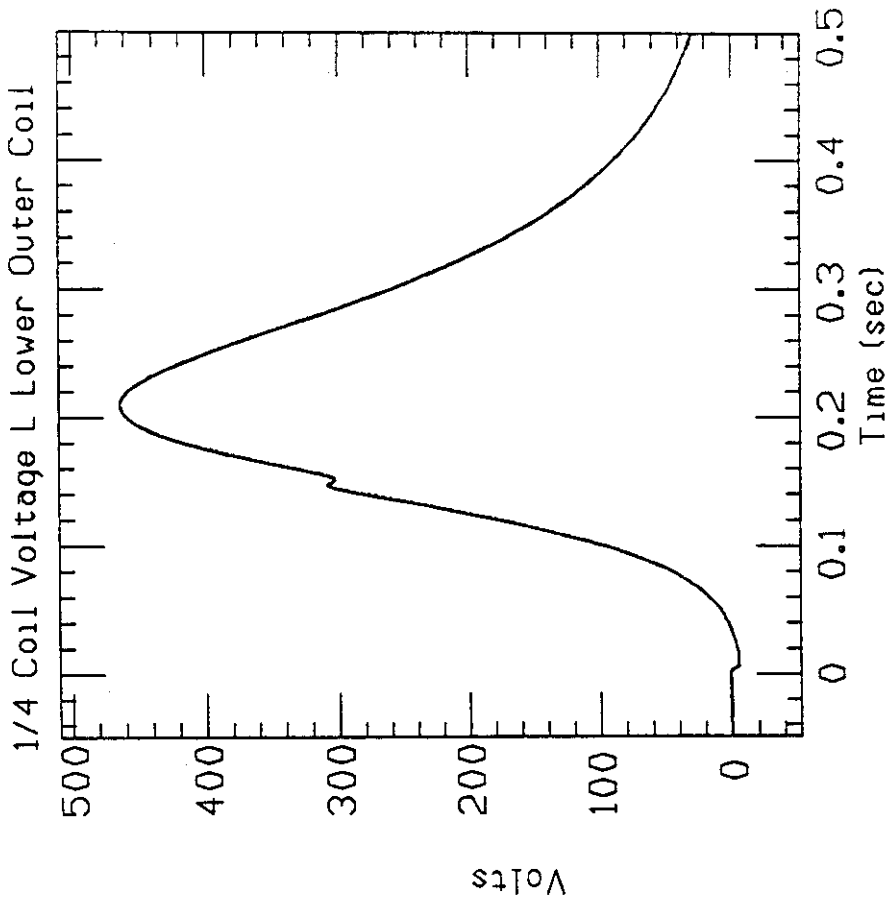


DD00012.QB082 Quench # 16 Current = 7051.  
S.C. # 1 t0 = -0.014 MIITs = 10.05  
Plot of Data Channel 110  
Ave. Initial Voltage :-3241E+01 +/- 0.6062E+01

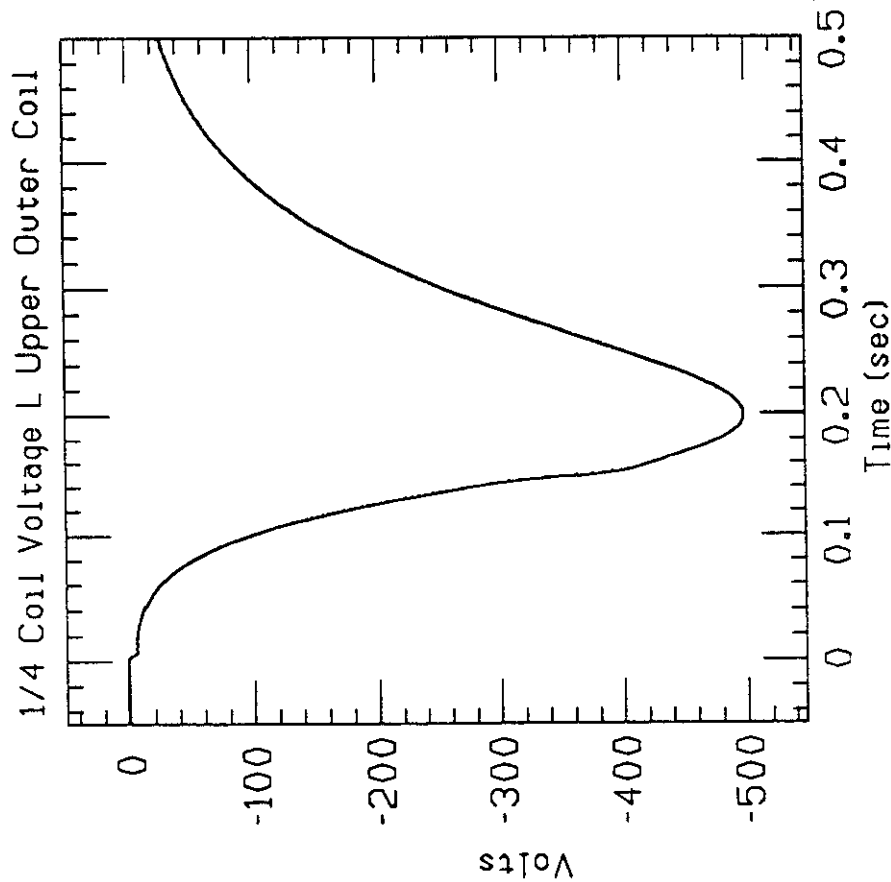


DD00012.QB082 Quench # 16 Current = 7051.  
S.C. # 1 t0 = -0.014 MIITs = 10.05  
Plot of Data Channel 101  
Ave. Initial Voltage :-6778E+01 +/- 0.1030E+02

Fig. 2.V.A.2

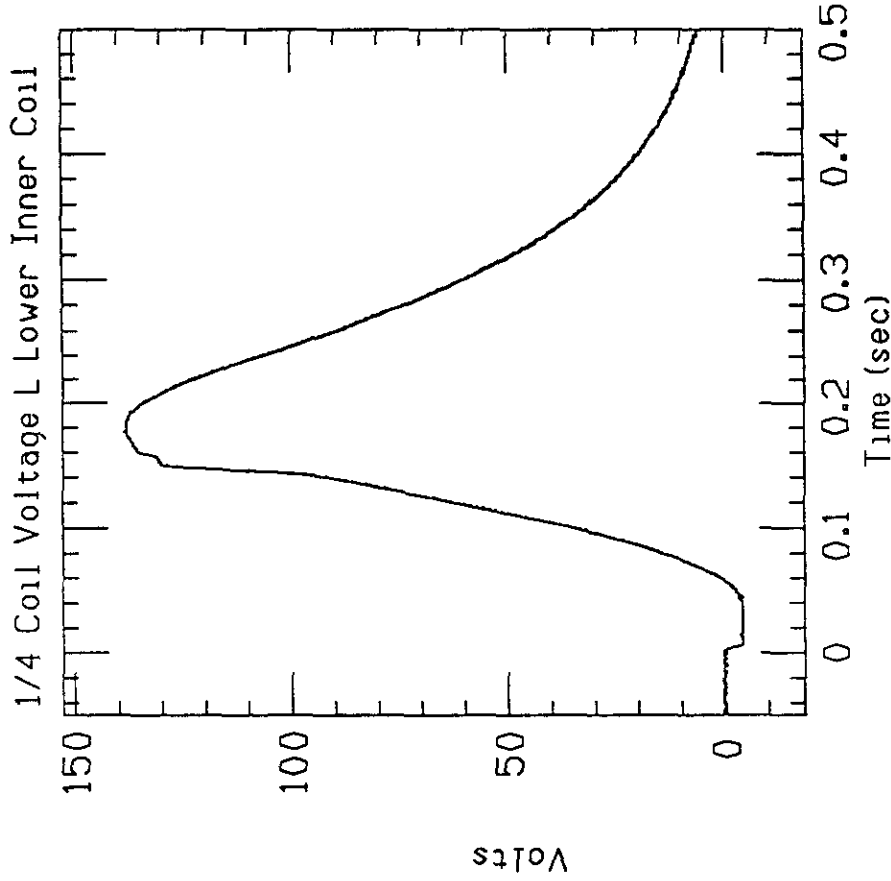


000012.08082 Quench # 16 Current = 7051.  
S.C. # 1 t0 = -0.014 MII's = 10.05  
Plot of Data Channel 112  
Ave. Initial Voltage :0.2279E+01 +/- 0.7182E+01

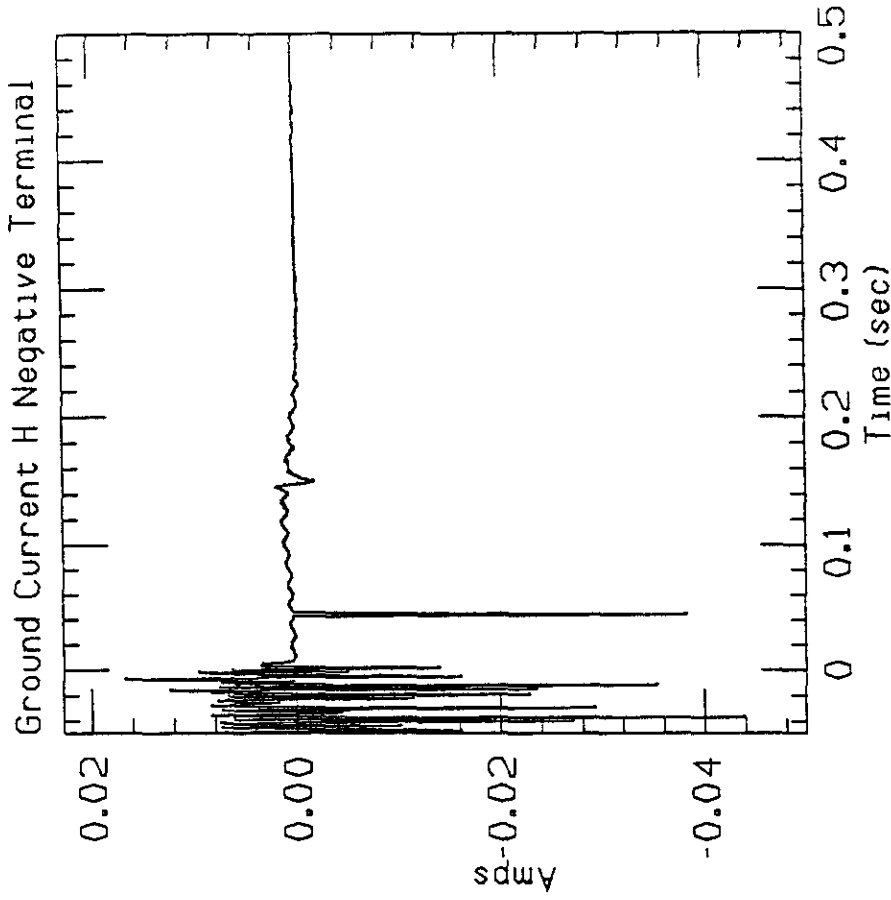


000012.08082 Quench # 16 Current = 7051.  
S.C. # 1 t0 = -0.014 MII's = 10.05  
Plot of Data Channel 111  
Ave. Initial Voltage :-0.4911E+01 +/- 0.9660E+01

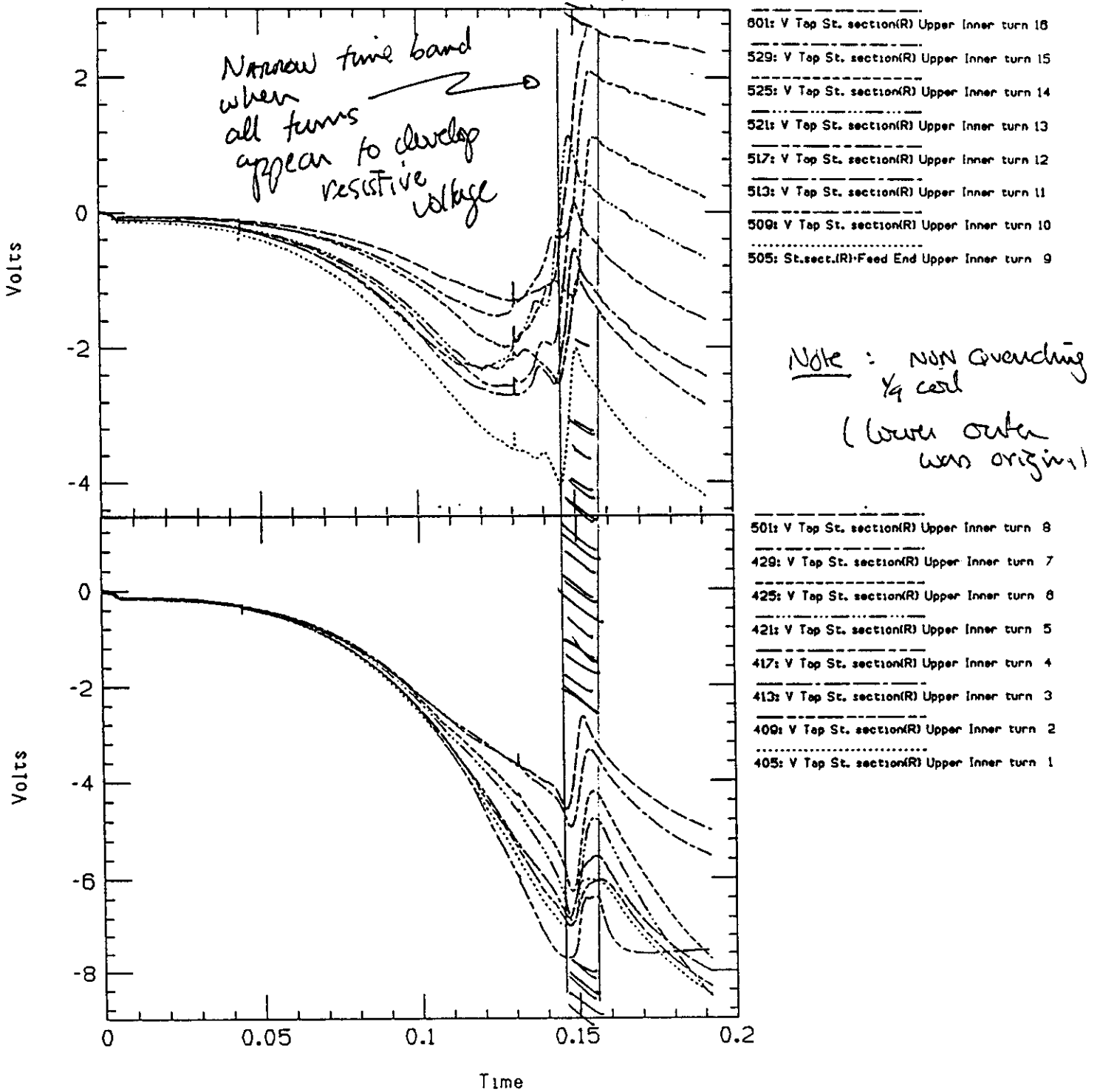
Fig. 2.V.A.3



000012.08082 Quench # 16 Current = 7051.  
S.C. #1 t0 = -0.014 MIITs = 10.05  
Plot of Data Channel 113  
Ave. Initial Voltage ::.5271E+00 +/- 0.2376E+01

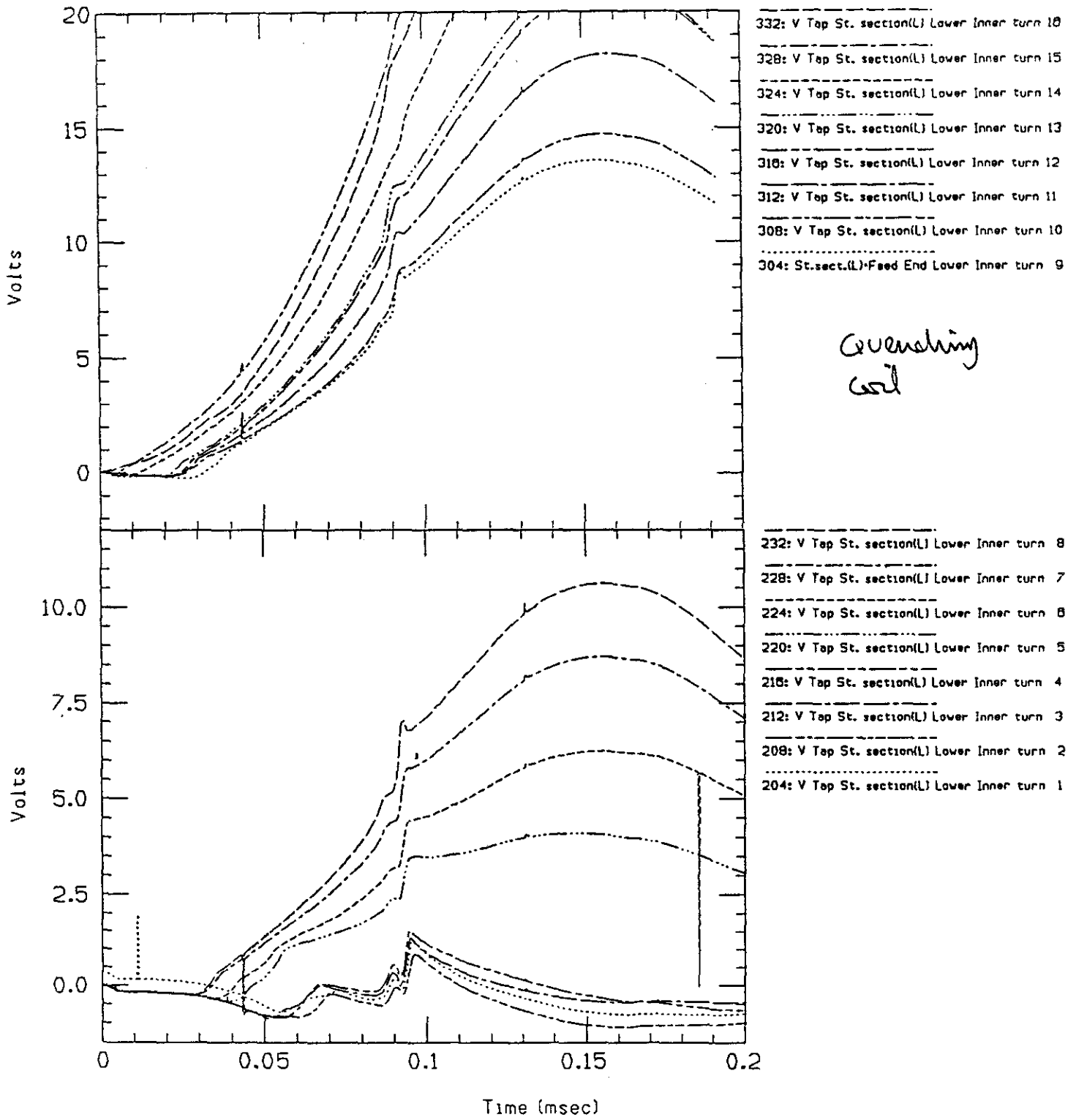


000012.08082 Quench # 16 Current = 7051.  
S.C. #1 t0 = -0.014 MIITs = 10.05  
Plot of Data Channel 118



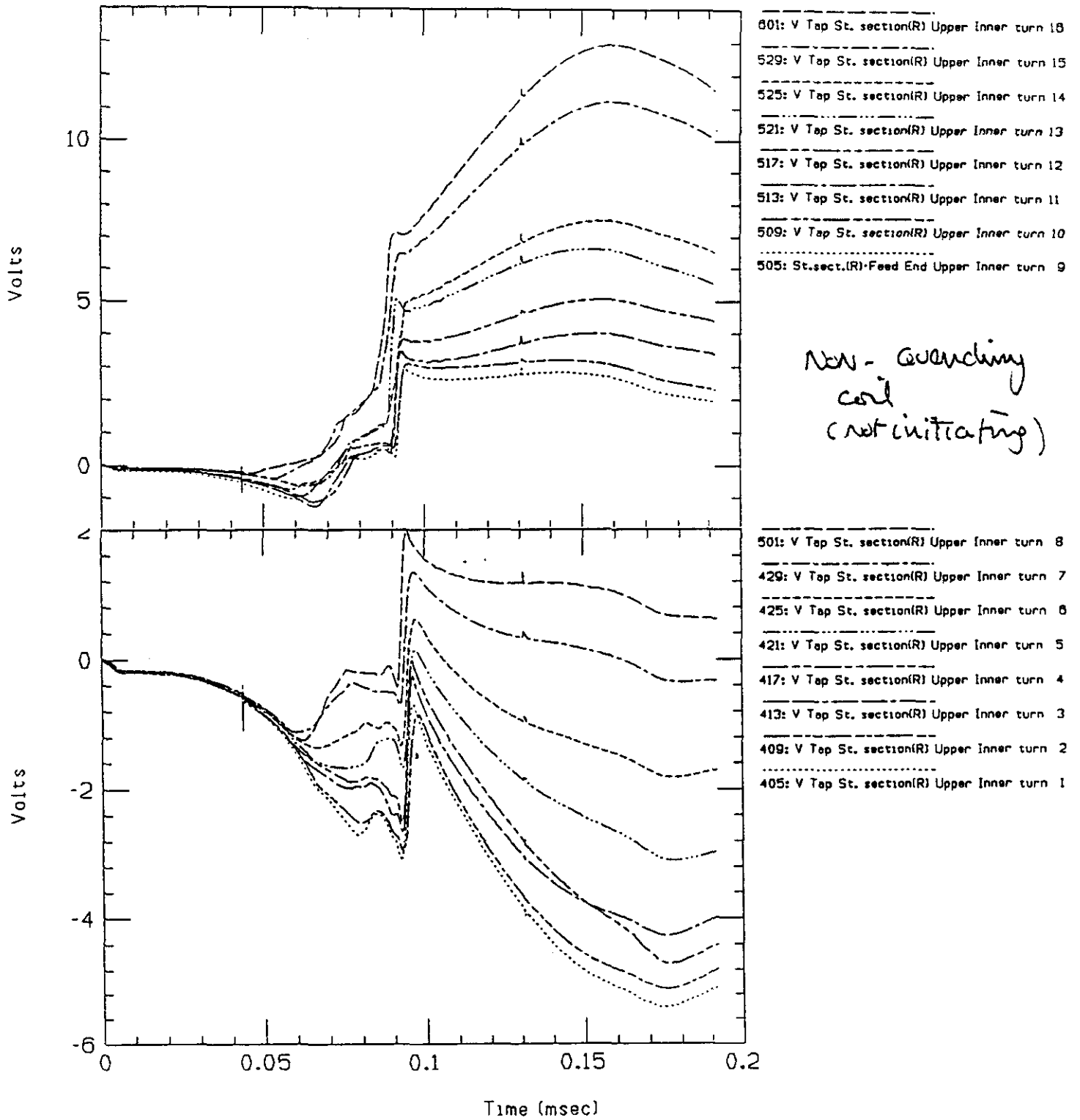
DD0012 Data File No. : 82 24-JUN-88 06:02:14 Quench No. : 0 Current - 7050.6

Fig. 2.V.A.5



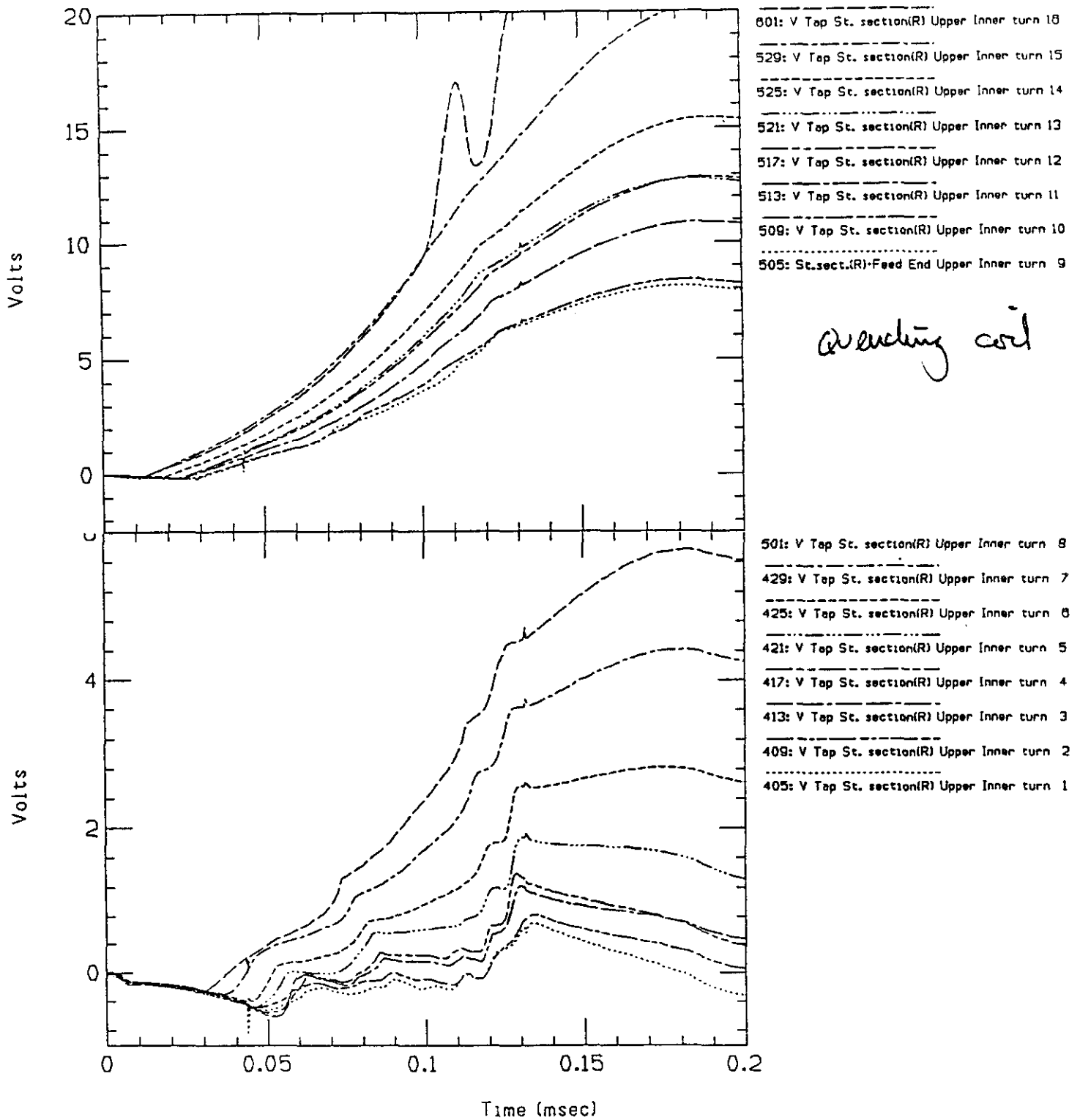
DD0012 Data File No. : 78 22-JUN-88 23:37:05 Quench No. : 13 Current = 7674.6

Fig. 2.V.A.6



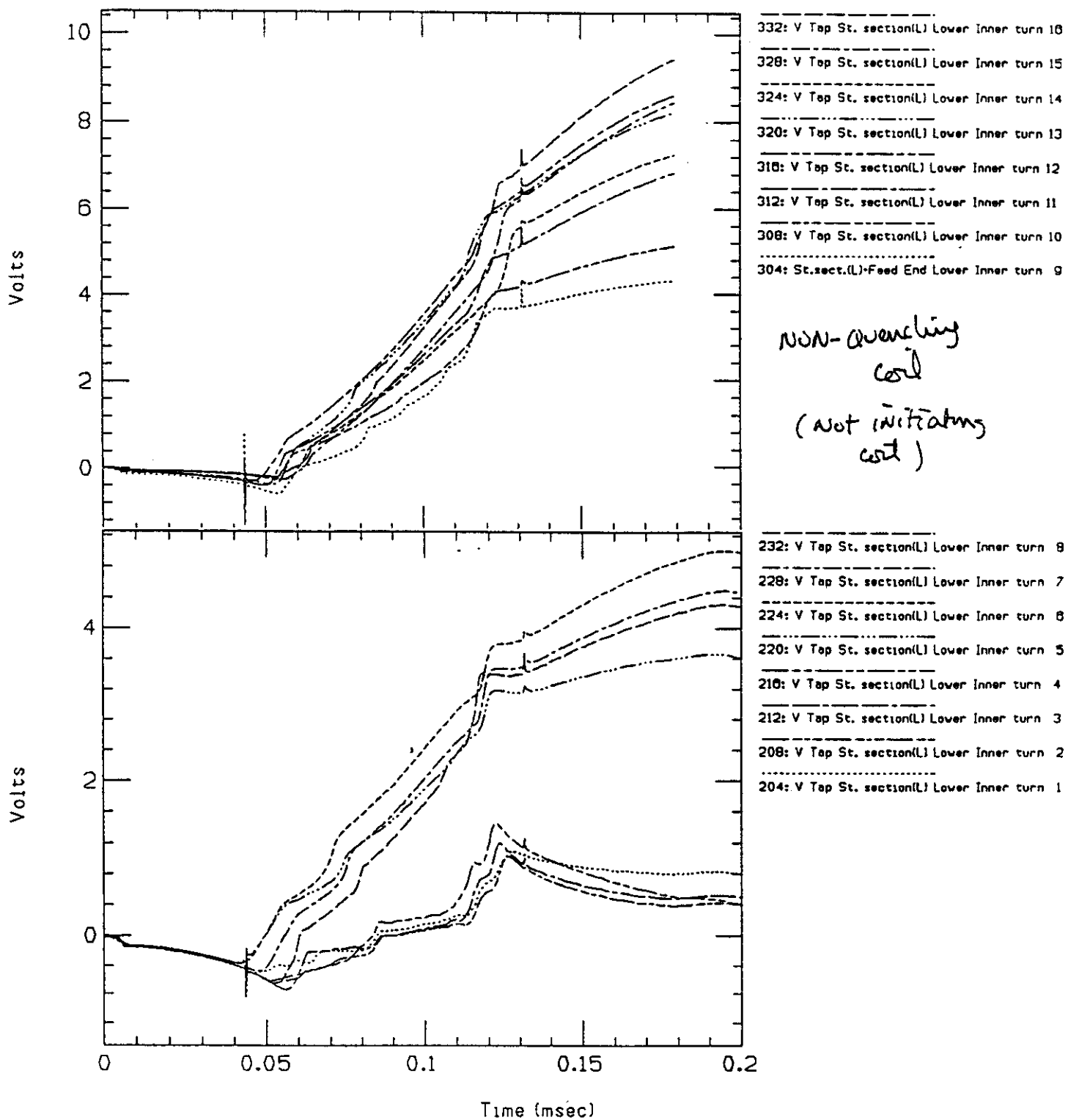
DD0012 Data File No. : 78 22-JUN-88 23:37:05 Quench No. : 13 Current - 7674.6

Fig. 2.V.A.7



DD0012 Data File No. : 18 6-MAY-88 17:09:14 Quench No. : 4 Current = 6548.8

Fig. 2.V.A.8



DD0012 Data File No. : 18 6-MAY-88 17:09:14 Quench No. : 4 Current = 6548.8

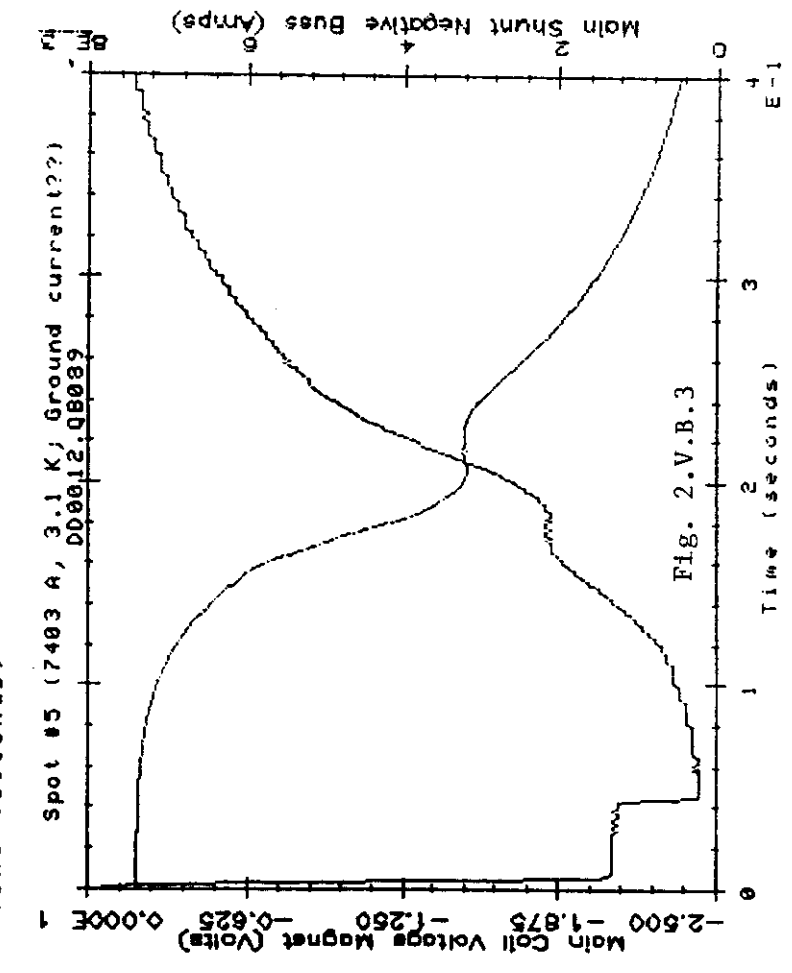
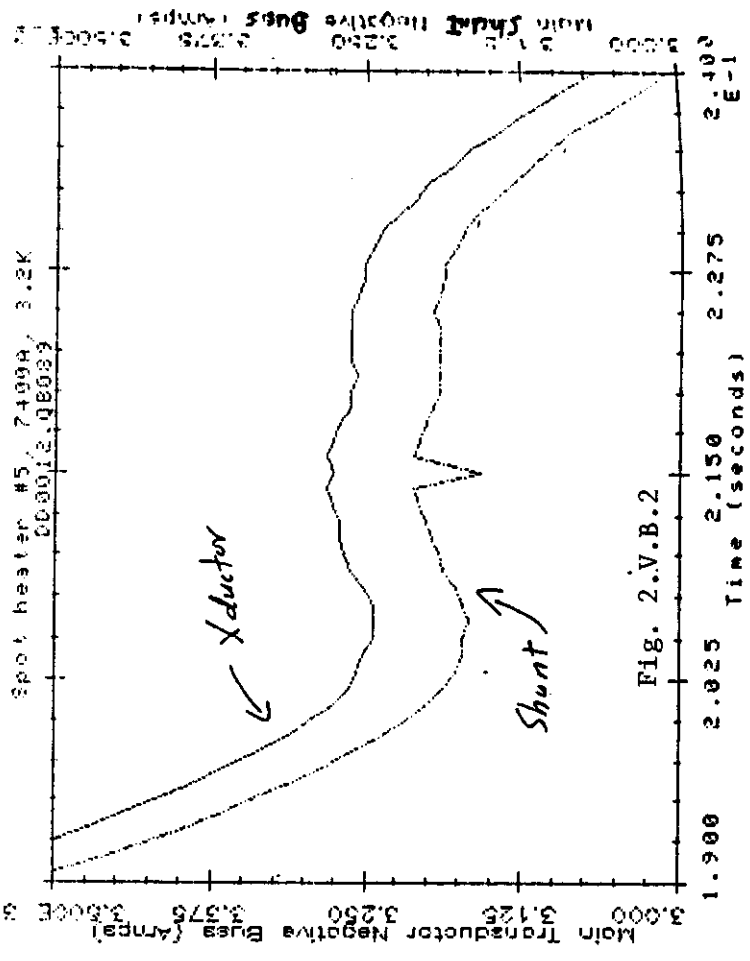
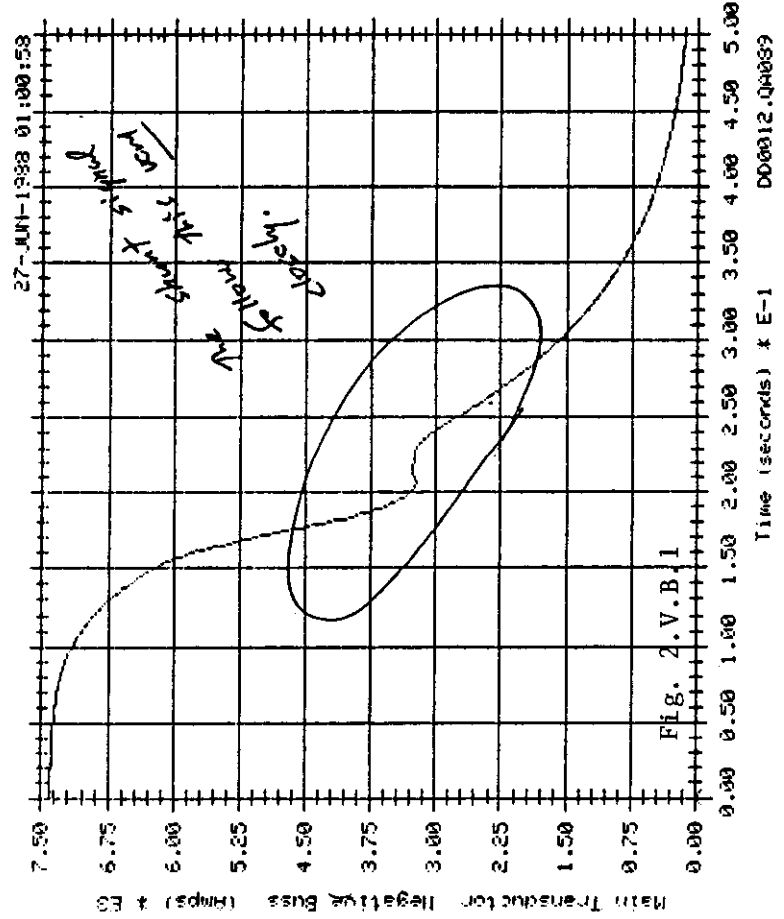
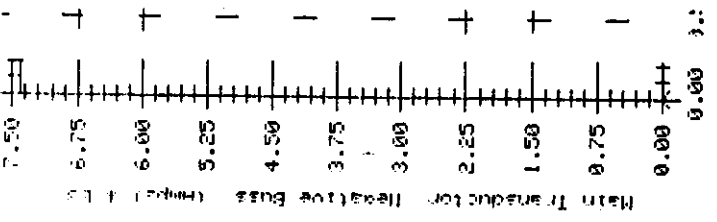
Fig. 2.V.A.9

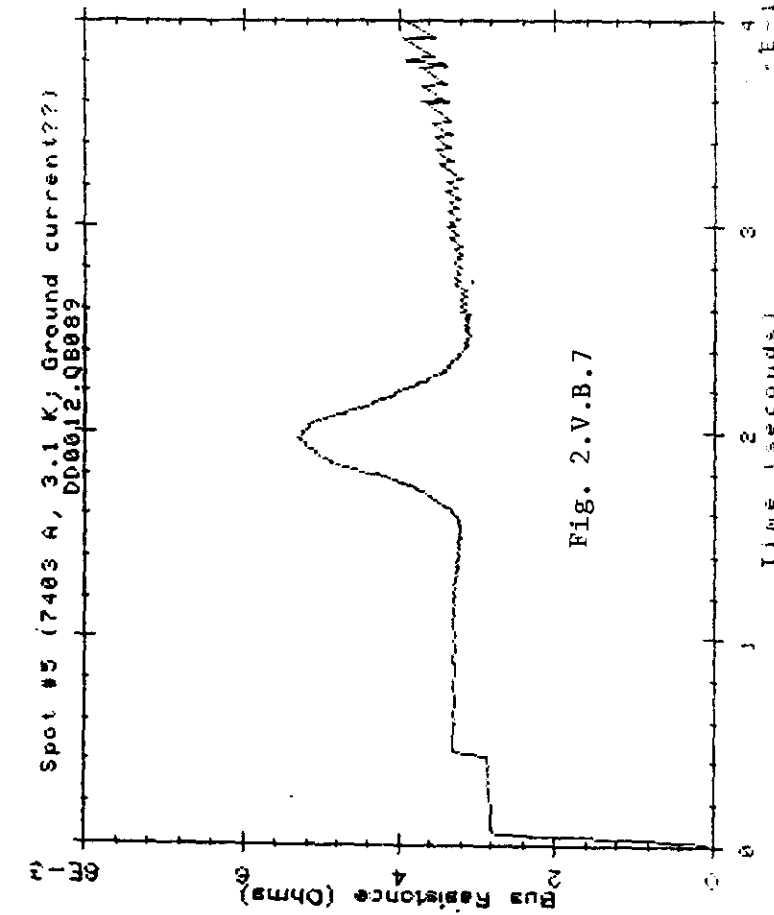
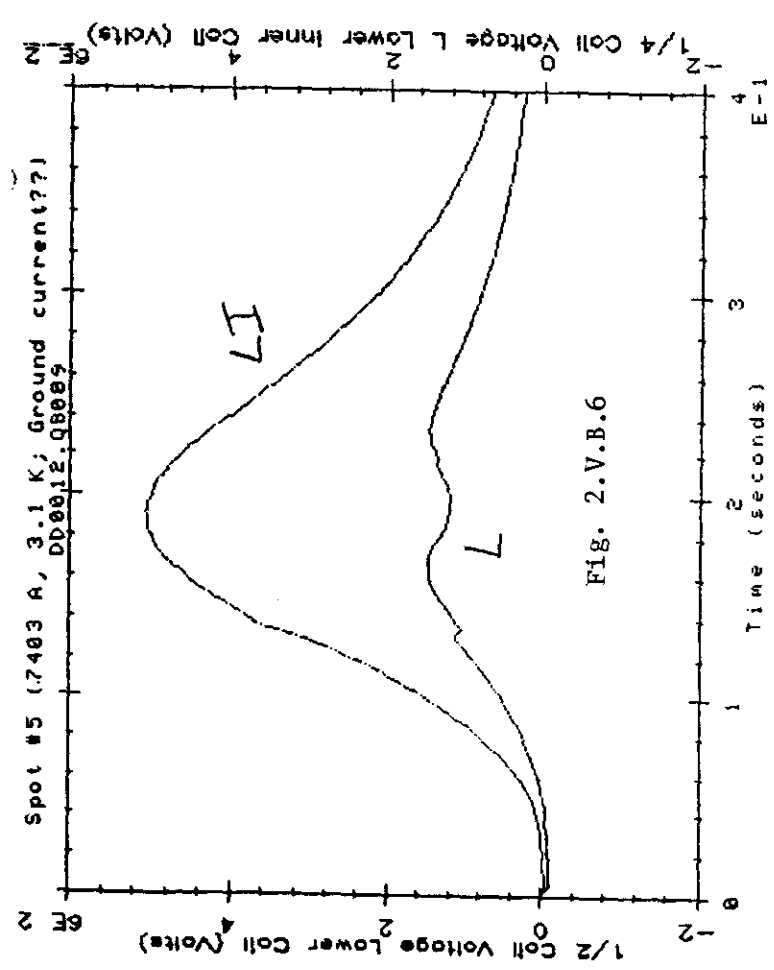
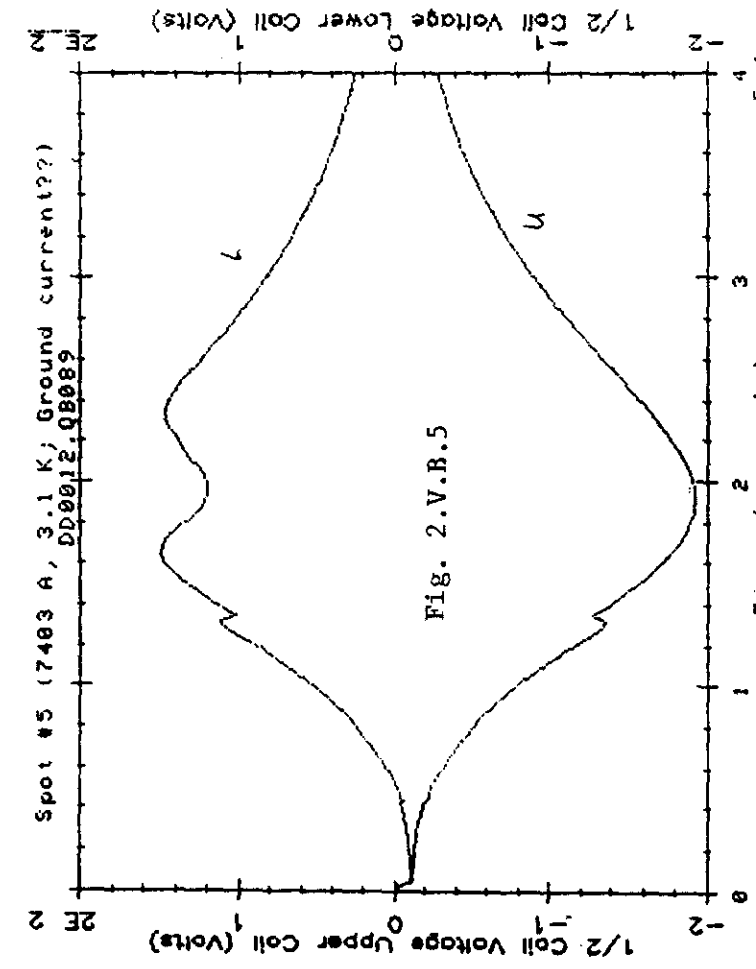
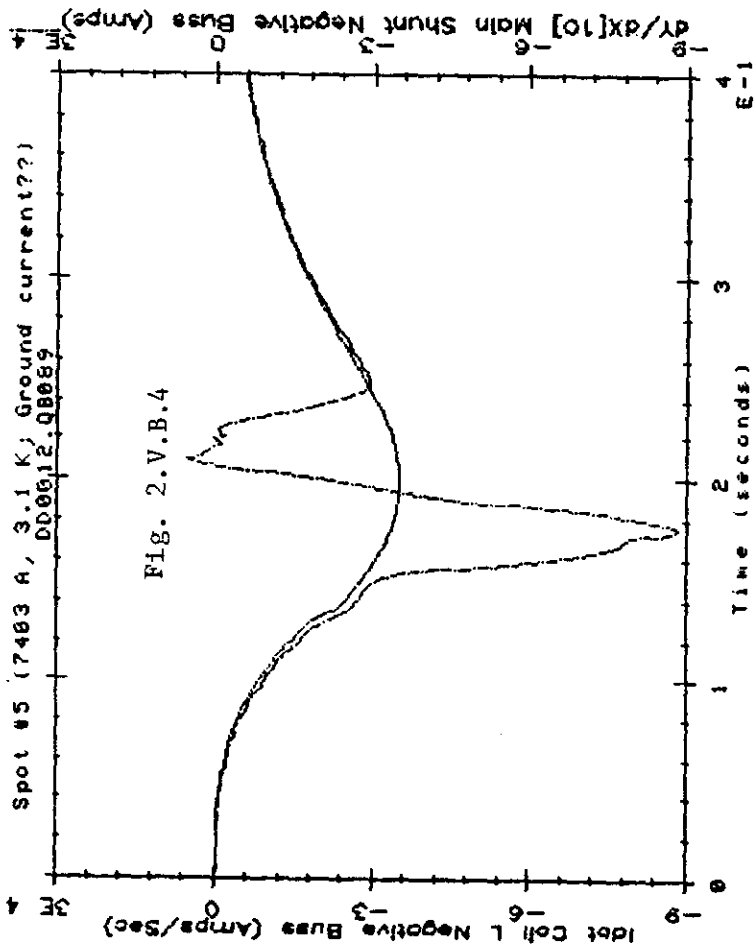
traces (Fig. 2), extending from about 200 to 250 ms after the quench was detected. It was also seen in the main coil voltage (Fig. 3), although at a slightly earlier time. It was not seen in the Idot coil, although the Idot trace follows the differentiated trace from the shunt well at other times (Fig. 4). The voltage trace from the lower half coil showed the irregularity (Fig. 5), but the lower inner quarter coil did not (Fig. 6), leading to the conclusion that the problem originated in the lower outer quarter coil. (The lower outer coil amplifier was not working, so this conclusion could not be directly confirmed.) Traces from the upper outer winding and the negative lead looked ok but the irregularity was seen in the buss (Fig. 7). The irregularity was seen in the low-gain trace of the ground current signal, but not in the high-gain trace (Figs. 8, 9).

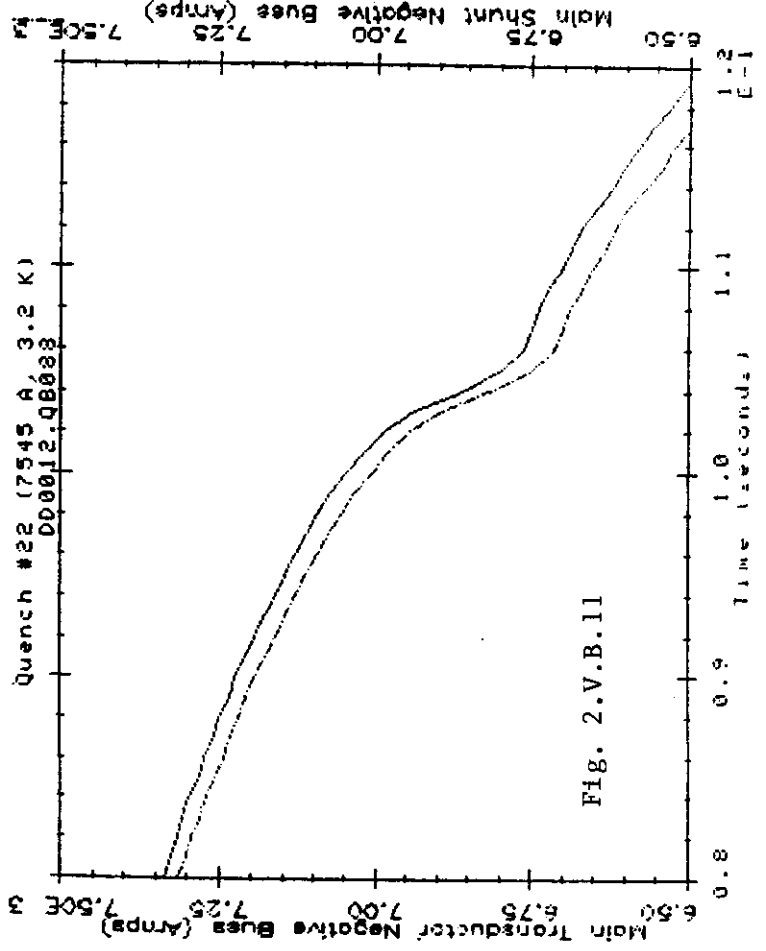
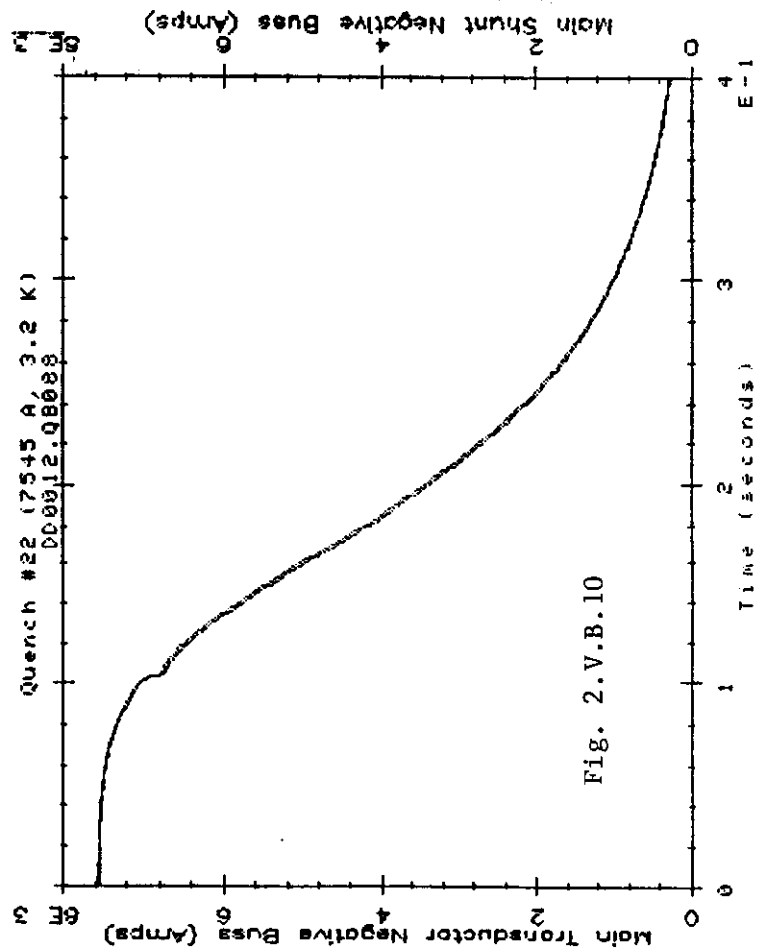
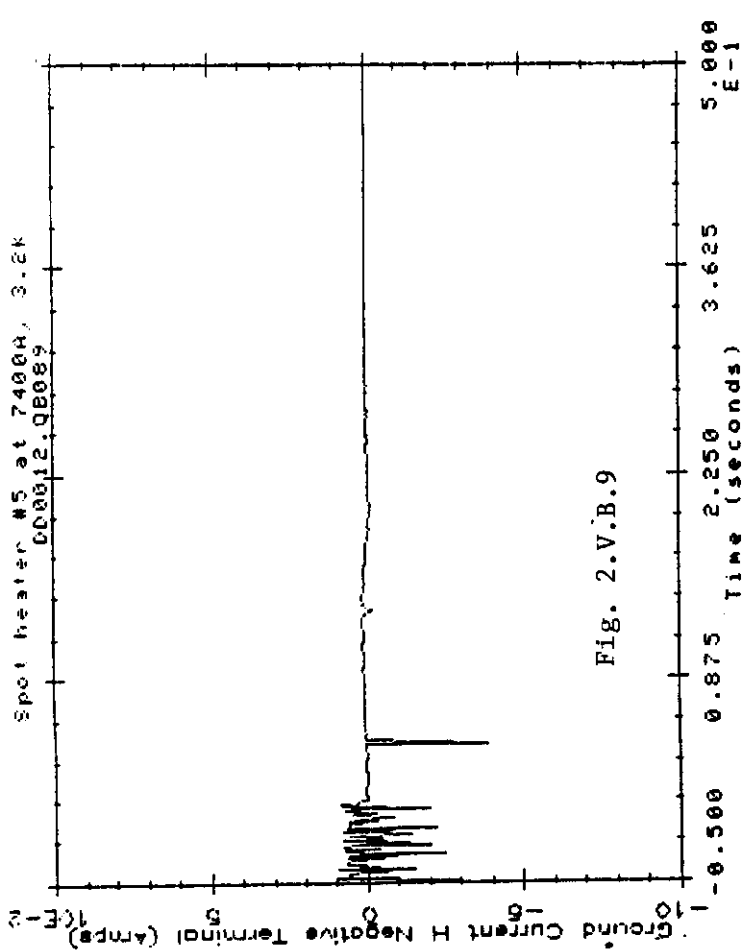
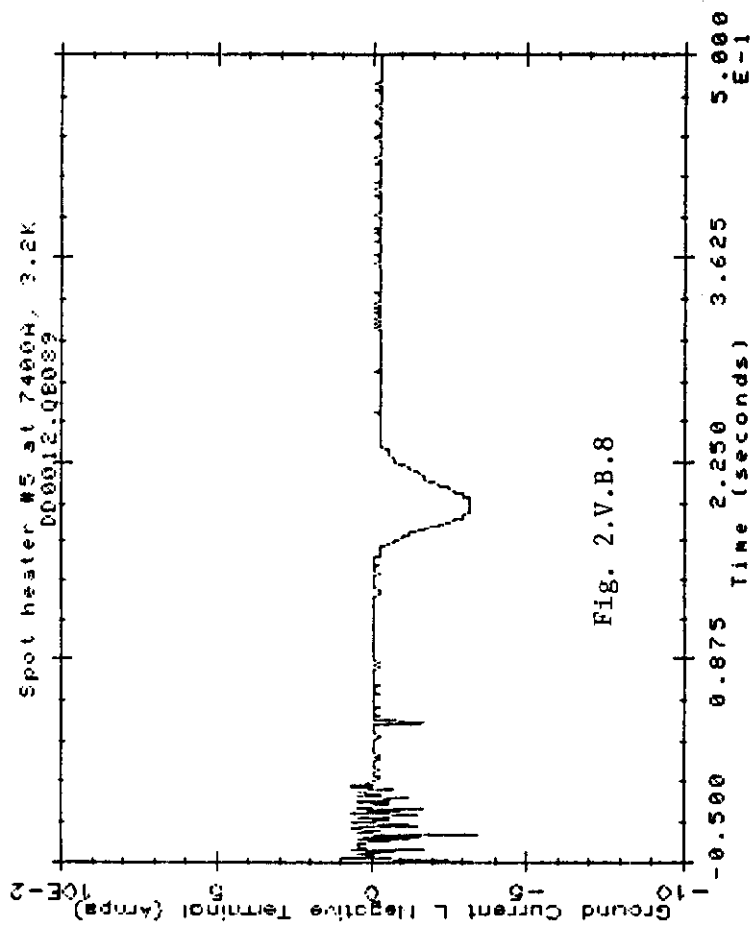
The magnet quench prior to the spot heater quench, spontaneous quench 22, was examined for the irregularity. The two current indicators showed a small irregularity at 105 ms (Figs. 10, 11). As with the spot heater quench, the Idot coil trace was smooth (Fig. 12). The buss resistance and ground current traces were smooth (Figs. 13, 14).

### C. Buss Voltage Pulses

Voltage pulses which exceeded the lead quench detection threshold and which originated in the buss occurred four times before the first spontaneous quench of the magnet and twice after that. Two examples are given in Fig. 2.V.C.1. The







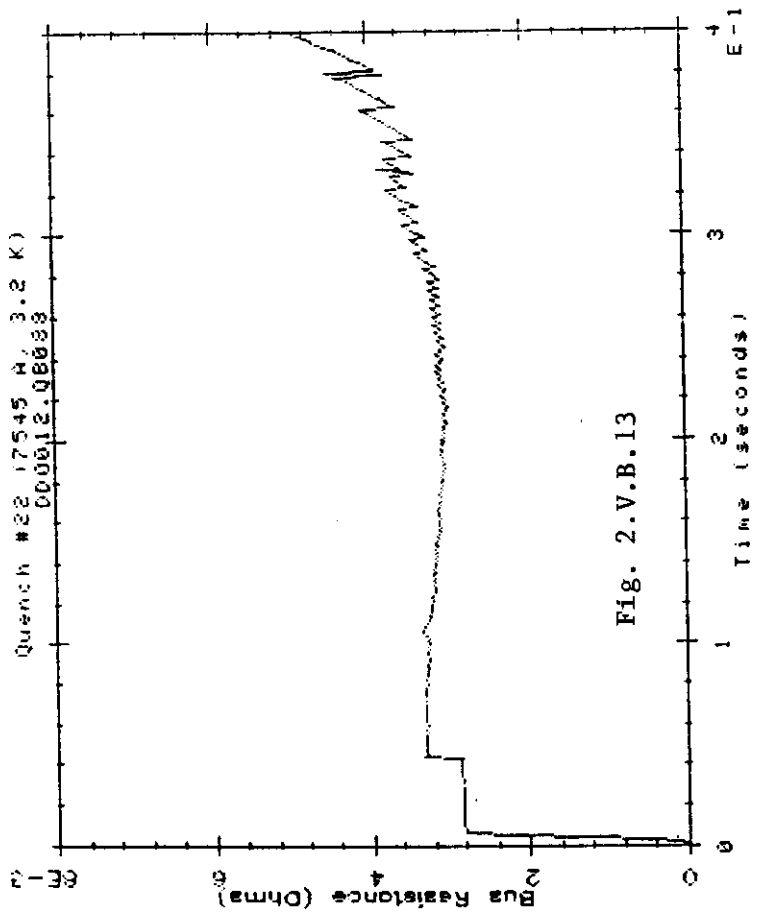


Fig. 2.V.B.13

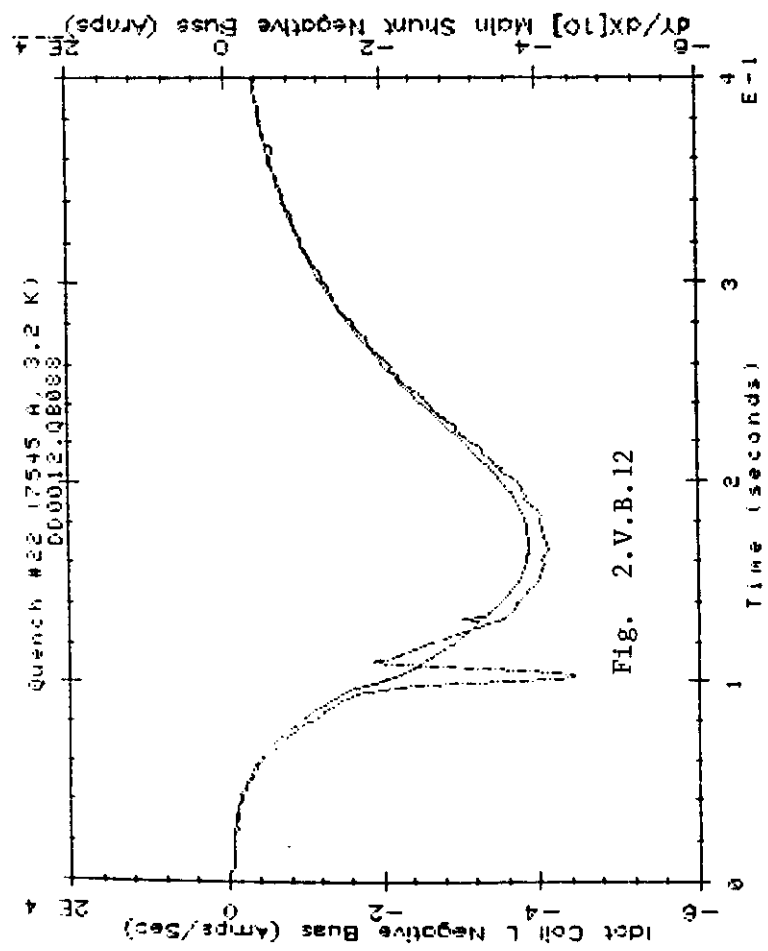


Fig. 2.V.B.12

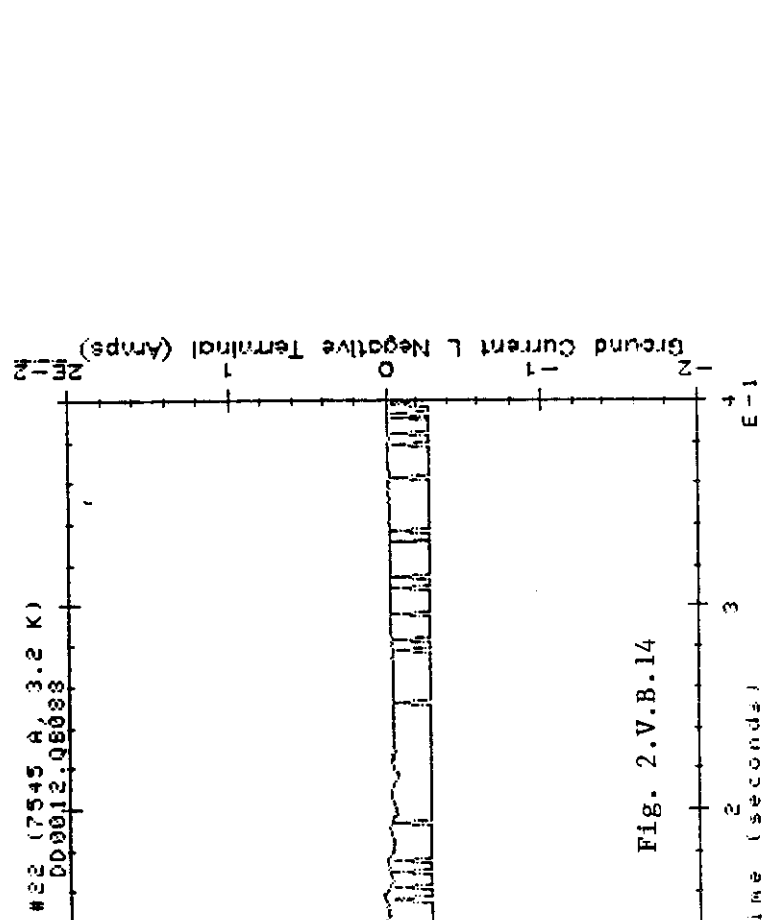
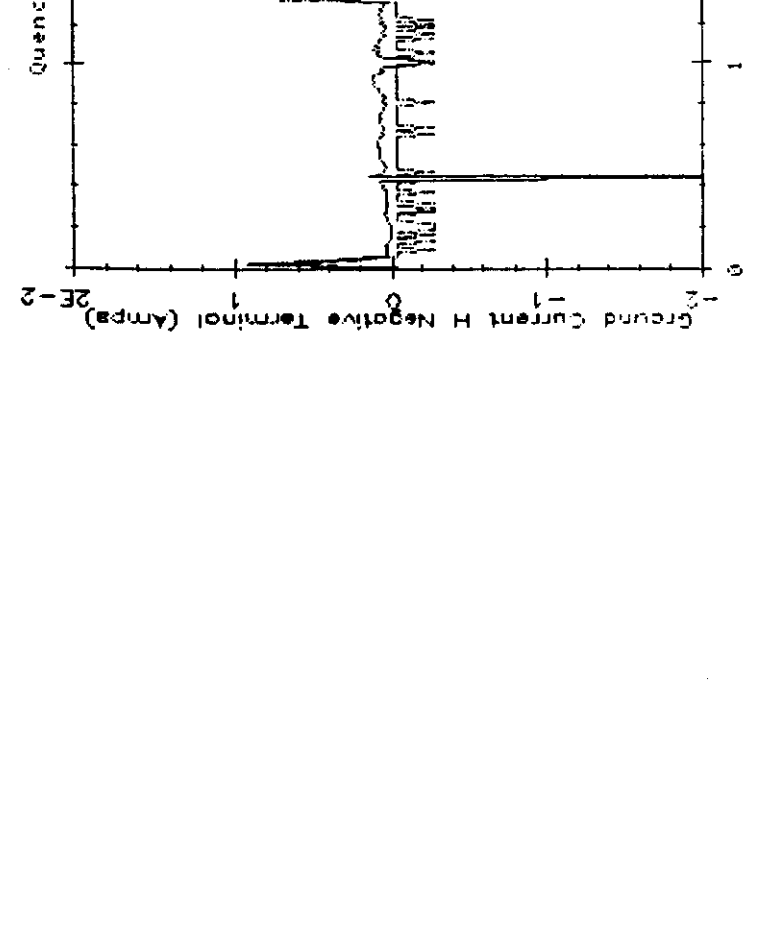
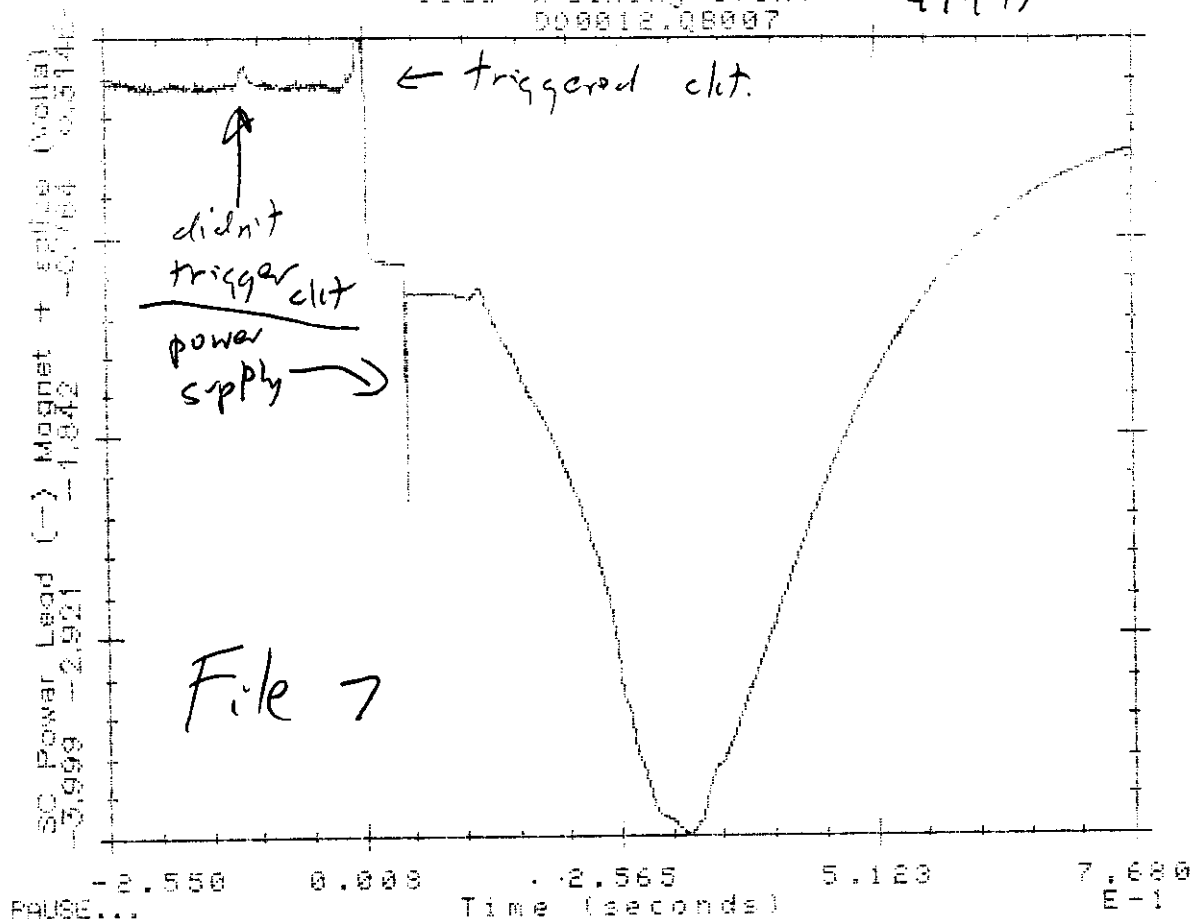


Fig. 2.V.B.14

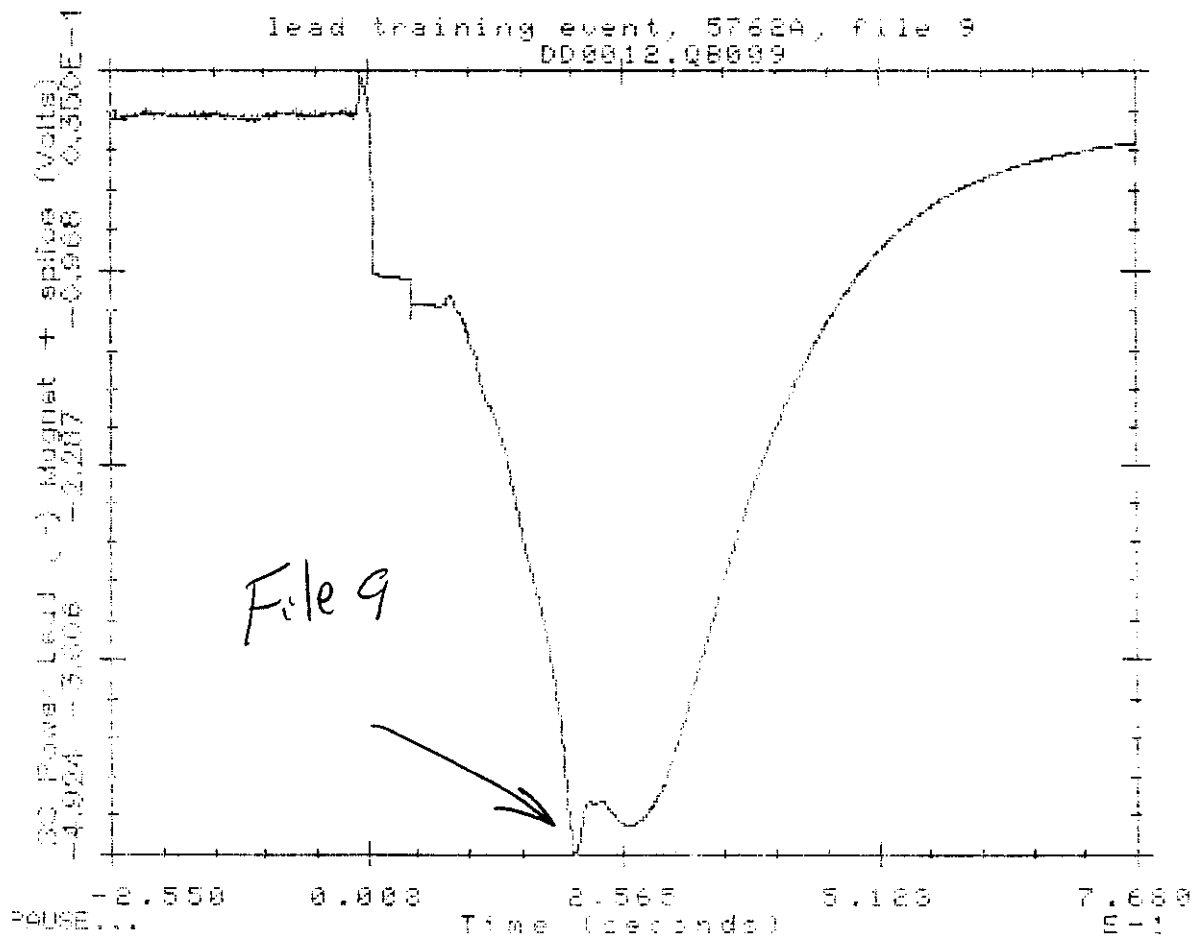


lead training event  
000012.08007

4947A



lead training event, 5762A, file 9  
000012.08009



example from file 7 also contains a smaller pulse about 100 ms before the trigger. Since the pulse occurs before the event, it was concluded that the voltage was due to conductor motion in the field (or something similar) and not to a quench (which would produce a monotonically increasing voltage on the scale displayed here).

The plot for file 9 shows another pulse about 200 ms after the trigger. These pulses could be generated if the lead relaxed all or part of the way as the field decreased.

A fix was put into place during the thermal cycle. The buss signal was separated from the others, filtered by an RC circuit with a 0.5 sec time constant, and compared to a signal from the Idot coil by a new quench detection circuit. This eliminated the problem from the test.

On the test stand, prior to the initial cooldown, it had been noted that the return end of the buss could be moved horizontally 1/8". A restraint was installed to restrict the motion. (DD14 allowed similar motion; DX did not.)

SECTION 3 -- DISASSEMBLY AND INSPECTION

## I. Coil Size Data

The disassembly provided the first opportunity for the use of a precise tool for measuring coil lengths. With the coil on the collaring press, only the upper half could be measured. The upper inner coil shortened by 0.373" and the upper outer outer by 0.117". Repeatability was at the level of a few mils.

Standard measurements of the size of the inner coils were made. Inner coil 17 had an average size (relative to a standard) of 16.4 mils before assembly and 14.3 mils afterwards. Inner coil 18 was 16.6 mils before and 15.3 mils afterwards. The size changes were fairly uniform along the length of the coils. (The outer coils have not yet been remeasured.)

## II. Inspection of Components

The strip heaters showed no signs of overheating, as were seen in DD10. (This was expected, since the power was reduced prior to testing DD12.)

In the ramp splice area, the cable insulation was abraded at the point where the cable leaves the G10 holder and enters the end region of the coil. On the lower half, which was the origin of the quenches which limited the magnet performance at reduced helium temperatures, the kapton was worn through. Also, stress lines were found in the G10 piece at a point where it had been hand-filed to accept the spliced cable. (This

piece has since been redesigned.)

The "venetian blinds," which shield the outer radius of the coils from the collars, showed little of the deformation at the midplane which was seen in DZ. (The deformation, referred to as "dimpling," was a ridge about 30-40 mils inward radially and azimuthally.) The pieces which were dimpled were shorter axially than the others, consistent with comments from the techs that the deformation probably occurred in venetian blinds which were reused.

No coil delamination was observed. This was in striking contrast to DD10, which was delaminated all along the length of inner coil turn 13.

The inner coil cable in the pole turn was displaced radially about 0.050" in the one-foot-long section next to the ramp-splice where the cable is not bonded to its neighbors. This was found in only one half.

In addition to the ramp splice, several other areas which were the source of occasional quenches were inspected. No irregularities were found, except for a few inches of the two turns adjacent to the ramp-splice in the outer coil, where the turns were not bonded on the outer radius. They were bonded on the inner radius.

The kapton midplane insulation passed the standard hipot test. The Z-cap at the pole showed no pinholes when inspected visually.